SAIMLAL – Sezione di Istologia ed Embriologia Medica

Scuola di dottorato in SCIENZE E TECNOLOGIE CELLULARI

XXV CICLO

c-FLIP$_L$ localizes

at the Endoplasmic Reticulum and Mitochondria-associated membranes

and regulates organelle morphology and ER-mitochondria crosstalk

Dottorando

MARINI ELETTRA SARA

Tutor

PROF. ELIO ZIPARO

2011-2012

“If we knew what it was we were doing, it would not be called research, would it?”

(Albert Einstein)

Sommario

ABSTRACT

Cellular FLICE-inhibitory proteins (c-FLIPs) regulate Death Receptor (DR)-induced apoptotic as well as non-apoptotic pathways, by modulating caspase-8 activation. Here we showed that the long isoform of c-FLIP unexpectedly controls the Endoplasmic Reticulum (ER) morphology and the physical and functional crosstalk between ER and mitochondria. Besides its previously described cytosolic localization, we observed that c-$FLIP_L$ is also retrieved at the ER and Mitochondria-associated membranes (MAMs), ER subdomains involved in the ER-to-mitochondria Ca^{2+} transport, lipid metabolism and ER stress-induced apoptosis. We demonstrated that the ablation of c-$FLIP_L$ in mouse embryonic fibroblasts (MEFs) specifically alters ER morphology, inducing ER-sheets proliferation and altering the luminal contiguity of this organelle. Re-introduction of c-$FLIP_L$ in c-$FLIP^{-/-}$ cells partially recovers these structural defects, therefore confirming the role of c-$FLIP_L$ in modulation of ER morphology. In agreement, we also reported that c-$FLIP^{-/-}$ MEFs show reduced expression of the ER shaping protein reticulon4 (RTN4), that is mainly known as regulator of ER biogenesis and dynamics. Furthermore, we observed that c-$FLIP_L$ ablation loosens ER-mitochondria juxtaposition. We demonstrated that functionally, c-$FLIP_L$ ablation lowers the cytosolic Ca^{2+}-increase evoked either by agonist stimulation or passive ER discharge. Furthermore, c-$FLIP^{-/-}$ cells are more resistant than their WT counterpart to cell death induced by the ER stress inducers thapsigargin and tunicamycin. Taken together, our findings suggest a novel role for c-FLIP as regulator of ER function and ER-mitochondria crosstalk.

INTRODUCTION

1. APOPTOSIS

Apoptosis was firstly described as physiologically controlled cell death in 1972 [1]. Apoptosis regulates several cellular processes, such as cell turnover and embryonic development, and its dysregulation is implicated in different disease states. Cells undergoing apoptosis exhibit a characteristic pattern of morphological changes, including cell shrinkage, membrane blebbing, DNA fragmentation and phosphatidylserine exposure [2]. The apoptotic process relies on the action of caspases, a family of aspartate-specific cysteine proteases, which cleave essential cellular proteins. Caspases initiate and execute cell death through a two-step mechanism in which initiator caspases (caspase-8, -9 and -10) cleave and activate the effector caspases (caspase-3, -6 and -7), which in turn cleave several distinct substrates to realize the apoptotic program [3]. Two major signaling pathways ensure proper execution of apoptosis, the extrinsic and the intrinsic pathway (Fig. 1) [4]. They are both initiated by the assembly of activating molecular platforms and the consequent recruitment and, local increase, in initiator caspases, therefore causing their activation through a process referred to as " induced proximity" [5].

1.1 The intrinsic pathway

The intrinsic pathway, also known as the mitochondrial pathway, is activated by stimuli that lead to mitochondrial outer membrane permeabilization (MOMP) and the release of proteins from the mitochondrial intermembrane space (IMS), including cytochrome *c*. In the cytosol, the cytochrome *c* engages APAF1 (apoptotic protease-activating factor-1) to form the apoptosome, an oligomeric signaling platform that brings together several molecules of caspase-9, the initiator caspase of the intrinsic pathway, enabling their autoactivation and cleavage of a large array of substrates. Apoptosis is a highly regulated process and various inhibitors specific for both the intrinsic and extrinsic pathway have been characterized. The most important regulators of mitochondrial apoptosis are members of the B-cell lymphoma protein-2 (BCL2) family. Among these, anti-apoptotic proteins such as Bcl-2 and Bcl-X_L prevent activation and oligomerization in the outer mitochondrial membrane (OMM) of the

pro-apoptotic members of BCL2 family Bid, Bax and Bak, which in turn promote the formation of large openings in the OMM and the release of cytochrome *c* and other pro-apoptotic factors from the IMS to cytosol [6].

1.2 The extrinsic pathway

The extrinsic pathway is initiated by the engagement of surface receptors of death receptor (DR) family by their ligands. All DRs belong to the tumor necrosis factor (TNF) receptor superfamily, and they are characterized by an extracellular domain consisting of a variable number of cysteine-rich repeats and a protein-protein intracellular interaction motif named death domain (DD) in their cytoplasmic tail [7]. The best characterized DRs are the apoptosis stimulating fragment (CD95/Fas), the TNF receptor 1 (TNFR1) and the TNF-related apoptosis-inducing ligand receptor 1 (TRAILR1) [8]. Triggering of CD95/Fas by its ligand CD95L/FasL induces the formation of a multimolecular complex of proteins termed death-inducing signaling complex (DISC) which consists of trimerized receptors, the Fas-Associated Death Domain (FADD) adaptor protein, the initiator caspase, procaspase-8 (or procaspase-10) and the cellular FLICE inhibitory protein (c-FLIP). FADD, which contains a C-terminal DD and an N-terminal death effector domain (DED), interacts via its DDs with the receptor, whereas DEDs are necessary to the homotypic interaction with procaspase-8, procaspase-10 and c-FLIP DEDs. At the DISC level, severale procaspase-8 molecules are recruited, thus favoring their auto-cleavage and activation and thereby leading to the triggering of the apoptotic signal. [9, 10]

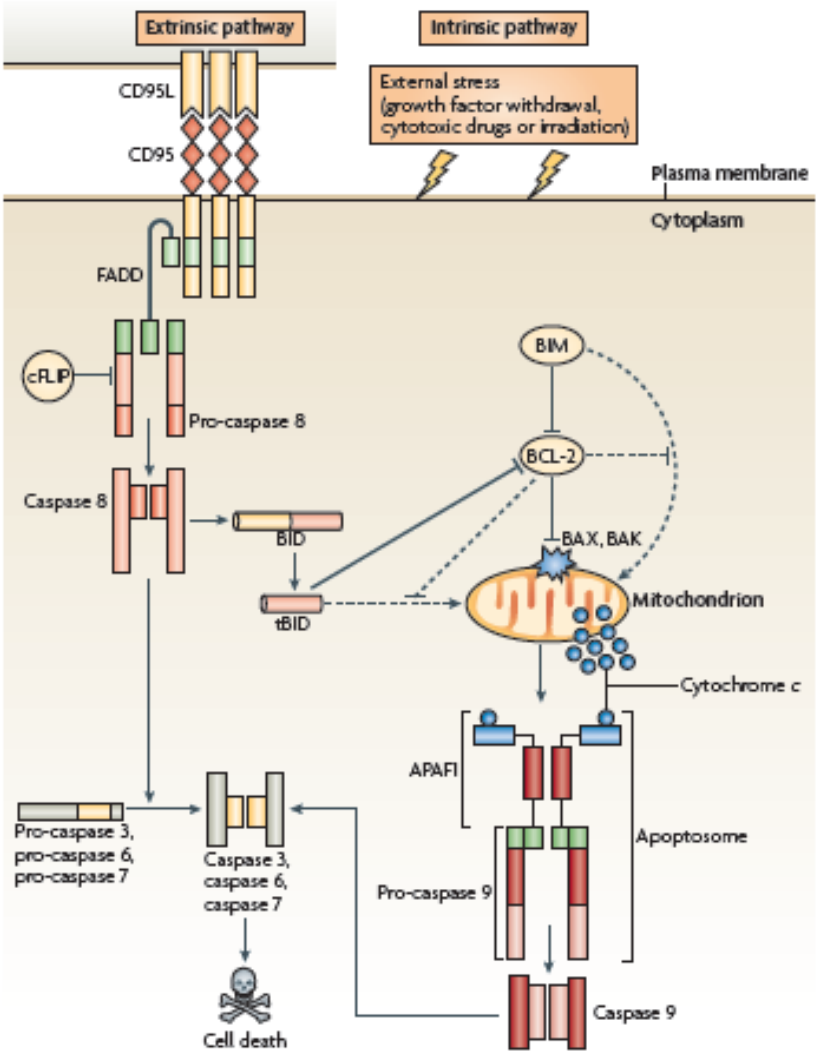

Figure 1: Intrinsic versus extrinsic apoptotic pathways [4].

2. CELLULAR FLICE INHIBITORY PROTEINS (c-FLIP)

2.1 Structure and function in apoptosis

After the characterization of caspase-8 and -10 and FADD as DED-containing proteins, other proteins structurally similar to the prodomain of caspase-8 were identified in several herpesvirus [11]. They are collectively known as viral FLIP inhibitory proteins (v-FLIPs). Shortly after their identification, human cellular homologues of v-FLIP were described by different groups and they have been termed cellular FLICE inhibitory protein (c-FLIP) [12, 13]. The gene encoding c-FLIP is called CFLAR (CASP8 and FADD-like apoptosis regulator). It is located on human chromosome 2q33, together with caspase-8 and -10, suggesting that these three genes arose by gene duplication [12]. Three different splice variants of c-FLIP have been described at the protein level: c-FLIP$_S$ (27kDa), c-FLIP$_R$ (25kDa) and c-FLIP$_L$ (55kDa) [12, 14]. All isoforms contain two DED motifs at their N-terminal, that is structurally similar to the N-terminal part of procaspase-8 (Fig. 2).

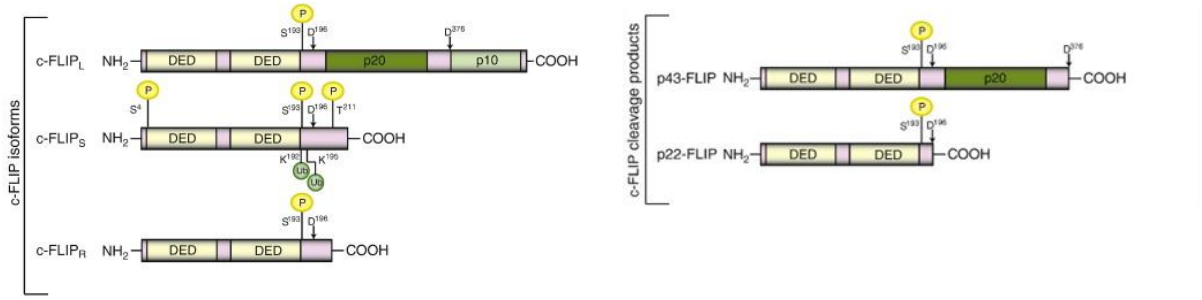

Figure 2: c-FLIP isoforms and cleavage products [10].

c-FLIP$_L$ is identical in length with caspase-8 and contains a caspase-like domain, that is catalytically inactive, at its C-terminal. By contrast, c-FLIP$_S$ and c-FLIP$_R$ present tandem DED motifs followed by a short and variable stretch of aminoacids at the C-terminal tail [10]. Besides full length isoforms of c-FLIP, cleavage products of this protein have been detected at the protein level as well. Active caspase-8 cleaves c-FLIP$_L$ at Asp-376 in the caspase-like domain, generating the so-called p43 fragment; procaspase-8 cleaves c-FLIP$_{S,R,L}$ on Asp-196, generating a cleavage product, called p22, containing the tandem DED motif. Active caspase-8 and procaspase-8 show mutually exclusive proteolytic specificity on these two cleavage sites [15, 16]. The three isoforms show differences in localization and functions. c-FLIP$_L$

localizes in the nucleus and cytoplasm, whereas c-FLIP$_{S,R}$ predominantly localize in the cytoplasm [17, 18]. All isoforms are recruited at the DISC in the early stages of death receptor-mediated apoptosis. At the DISC, c-FLIP interacts with FADD, preventing the interaction between FADD and procaspase-8 and blocking the transduction of the apoptotic signal. It has been reported that all isoforms strongly associate with FADD through their DED motifs, whereas the caspase-like domain of c-FLIP$_L$ is by contrast necessary to the interaction with both procaspase-8 and active caspase-8 [12, 19]. Although v-FLIP and c-FLIP$_{S,R}$ are widely accepted as anti-apoptotic proteins, the role of c-FLIP$_L$ is still unclear. Indeed, besides its anti-apoptotic function, a pro-apoptotic role depending on caspase-8:c-FLIP$_L$ ratio has also been reported (Fig. 3) [20-22]. At lower, physiological concentrations, c-FLIP$_L$ heterodimerizes with both procaspase-8 and caspase-8. Heterodimerization allows the allosteric activation of procaspase-8, promoting the initial processing of caspase-8, but restricting its activity below a threshold such that the fully active caspase-8 is not formed. Moreover, caspase-8/c-FLIP$_L$ heterodimers are confined to the DISC and process only proximal substrates such as the receptor-interacting protein (RIP) and c-FLIP$_L$ itself, which is cleaved to the p43 fragment. These findings suggest that a complete block of caspase-8 activity is not advisable, and hypothesize alternative apoptosis-independent activities of caspase-8. At moderate expression levels, found in some tumors and cell lines, c-FLIP$_L$ acts as an inhibitor of DR-mediated apoptosis. Conversely, when highly overexpressed, c-FLIP$_L$ results cytotoxic by itself, probably through the association with caspase-8 outside the DISC.

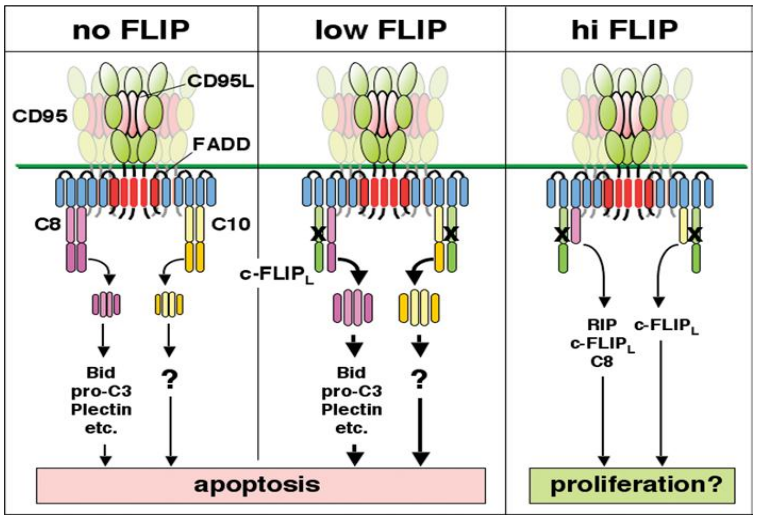

Figure 3: Controversial functions of c-FLIP$_L$ [23].

2.2 Non apoptotic function of c-FLIP

In addition to their function in apoptosis signaling, c-FLIP, FADD and procaspase-8 are also critical mediators of cell survival and proliferation, particularly in lymphocytes. Ablation of any of these genes yields embryonic lethality in mice. Knockout mice for c-$FLIP_L$ have defects similar to FADD and caspase-8 knockout and are characterized by heart failure and death at embryonic day 10.5, thus suggesting a potential pro-apoptotic role of c-$FLIP_L$ [25]. A common non-apoptotic function for DED proteins has been also confirmed in conditionally depleted, murine T cell, which resulted incapable to proliferate upon T-cell receptor stimulation (Reviewed in [24]). In accordance, both c-$FLIP_L$ and partially active procaspase-8 can promote the NF-kB pathway, inducing cells survival and proliferation [26].

Heterodimerization of the two proteins and caspase-b mediated cleavage of c-FLIP to form the p43 and p22 fragments could explain NF-kB induction. In fact, both cleavage products could interact with proteins regulating the NF-kB pathway, therefore strongly promoting NF-kB activation (Fig.4) (Reviewed in [24]).

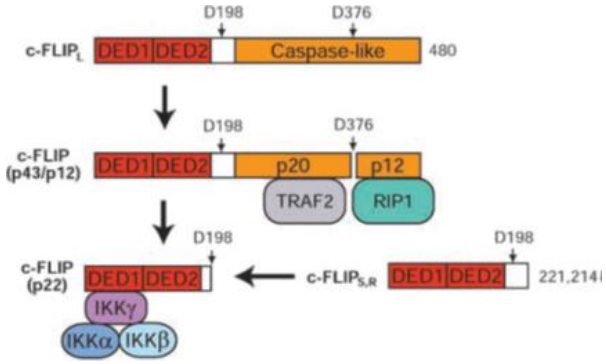

Figure 4: Proteolytic cleavage of c-FLIP by procaspase-8 and its role in NF-kB pathway [24].

3. TYPE I AND II CELLS IN THE FAS SIGNALING

Although the extrinsic and intrinsic pathways act independently, it is now clear that in some circumstances the DRs pathway relies on the amplification of death signals mediated by the mitochondrial pathway. On the base of the dependence of the death receptor-mediated apoptotic signal on the intrinsic pathway, Fas-expressing cells and tissues are classified as type I or II [27]. Type I cells, such as lymphocytes, bypass the need for mitochondrial amplification in Fas-mediated apoptosis by producing large amounts of DISC and therefore activating caspase-8, which can in turn directly activate the executioner caspases. By contrast, type II cells generate very little active caspase-8 at the DISC and they completely rely on the intrinsic pathway. Indeed, the small quantity of active caspase-8 is unable to induce apoptosis, but is sufficient to cleave the pro-apoptotic BH3-only protein of the BCL2 family Bid. Truncated Bid (tBid) translocates to mitochondria where it activates other two pro-apoptotic member of BCL2 family Bax and Bak, inducing mitochondrial permeabilization, which ultimately enhances the apoptotic signal [28].

3.1 Lipid rafts involvement in modulation of Fas signaling

Recently, this model has been refined by the finding that, following receptor stimulation, members of TNFR family are recruited to membrane subdomains called lipid rafts (LRs). The different efficiency of Fas signaling in type I and II cells can hence depends on receptor submembrane localization [29]. In particular, it has been demonstrated that in type I cells, Fas partially resides constitutively in LRs, while it is excluded from these microdomains in type II cells. LRs could therefore sensitize type I cells by acting as signaling platforms where Fas receptor is partially pre-associated, thus easily recruiting and activating DISC components. By contrast, in type II cells Fas is not pre-associated, but it is recruited to, after stimulation [30]. Proteins that are N-myristoylated and/or S-palmitoylated partition into membrane rafts. It has been hence hypothesized that Fas palmitoylation on cysteine 199 is involved in the recruitment of the receptor into LRs and in its efficient aggregation, that is a mandatory step in triggering cell death [31].

More recently, the ability of other DISC components such as caspase-8 and c-$FLIP_L$ to redistribute to LRs, after T cell activation, has been reported [32]. This model suggests that TCR-induced caspase-8 activation occurs in a sequestered environment that limits the degree

of caspase-8 activation as well as restricts the cleavage of caspase-8 substrates to those not necessarily involved in cell death execution. The occurrence of Fas signaling in sequestered membrane LRs could influence the efficiency of signaling and limit caspase-8 activity to local substrates, therefore contributing to explain the controversial role of DRs signaling and DISC components in regulation of both apoptosis and proliferation.

4. LOCAL COMPLEXES OF CASPASE-8 ACTIVATION

In the last years, the importance of intracellular protein complexes and their localization in modulating cellular functions has emerged. Regarding components of the DISC, it is now clear that both FADD and procaspase-8/caspase-8 can associate to intracellular organelles such as mitochondria and endoplasmic reticulum (ER), where they seem to be recruited in local complexes to regulate not only the apoptotic response following DRs engagement, but also ER stress and ER-mitochondria crosstalk.

4.1 Recruitment on mitochondrial signaling platforms: the role of cardiolipin

Even though procaspase-8 and caspase-8 were mostly considered cytosolic proteins, their association to mitochondrial outer membrane (OMM) was also described [33, 34]. More recently, it has been demonstrated that the mitochondrial phospholipid cardiolipin (CL) induces caspase-8 accumulation and processing at the mitochondrial outer membrane [35]. CL is a mitochondrial, anionic phospholipid, that is enriched in internal mitochondrial membrane (IMM) and at the contact sites between the inner and outer membranes of these organelles. CL has been shown to associate with members of the apoptotic machinery, such as cytochrome *c* and members of BCL-2 family (Reviewed in [36]). Furthermore, CL serves as docking site for tBid on the mitochondrial membrane [37] and regulates Bax oligomerization and MOMP [38]. In type II cells CL is necessary to the formation of an apoptotic signaling complex where several molecules of procaspase-8 cluster and are activated by proximity upon Fas stimulation [35]. This "compartimentalized" processing of caspase-8 indicates that the activation of a caspases-cascade on local signaling platforms such as mitochondria, could promote the cleavage of specific substrates where they are necessary: along CL docking sites on mitochondria, caspase-8 activates Bid directly on the surface of its target organelle, thus promoting Bax and Bak oligomerization, cytochrome *c* release and apoptosis (Fig. 5) [39].

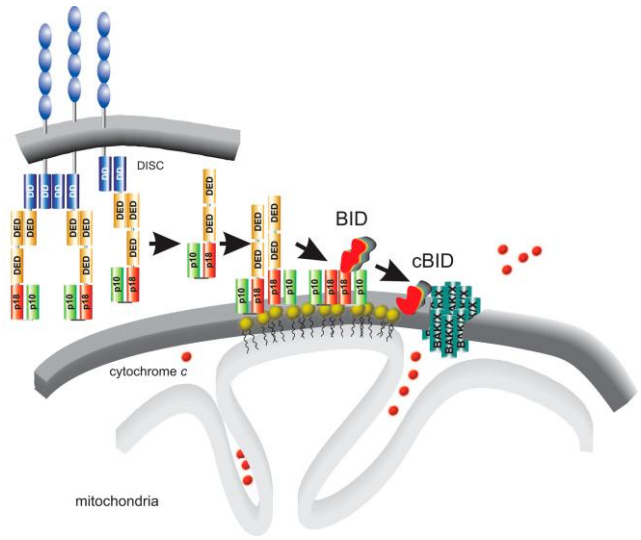

Figure 5: Localized production of active, cleaved Bid on cardiolipin platforms [39].

4.2 Recruitment on ER signaling platforms: the role of Bap31

Among locally-cleaved caspase-8 substrates, it has been identified the ER resident protein Bap31 [40]. Bap31 is an ER integral membrane protein, that binds to nascent membrane proteins in transit between ER and *cis*-Golgi. In response to the oncogenic adenovirus E1A and Fas ligand, Bap31 forms a signaling complex in the ER including Bcl-2/Bcl-X_L and the isoform of procaspase-8, procaspase-8L [40, 41]. The cytosolic tail of Bap31 indirectly interacts with caspase-8, that in turn, cleaves Bap31 on two cleavage sites. Although the full length Bap31 acts as a direct inhibitor of caspase-8, when it is cleaved by this caspase, the truncated, membrane-embedded p20, fragment by contrast acts a potent apoptosis inducer. BCL2-family proteins are localized both at the ER and mitochondria [42] and the association of Bap31 with both procaspase-8 and Bcl-2/Bcl-X_L raises the possibility that the Bap31 complex in the ER cooperates with mitochondria in the modulation of a Bcl-2-regulated caspase-cascade. In agreement, the caspase-resistant Bap31 (crBap31) provides resistance to Fas-mediated apoptosis, preventing mitochondrial remodeling and cytochrome *c* release, although procaspase-8 and Bid activation seems not to be influenced [43]. Cleavage of Bap31 at the ER therefore, appears to support the mitochondrial step following Fas stimulation, suggesting that events at the ER can influence those mitochondrial modifications which sustain apoptotic responses (Fig. 6). More recently, it has been observed that the p20 fragment

mediates the Ca^{2+}-dependent ER-mitochondria crosstalk, suggesting that efficient Fas signaling requires Ca^{2+}-release from the ER [44]. In fact, after Fas stimulation, the p20 fragment promotes mitochondrial fragmentation mediated by the dynamin related protein 1 (Drp1). However, Bax activation and cytochrome *c* release are delayed, thus suggesting that Ca^{2+}-dependent signals from ER sensitize mitochondria to the following caspase-8 mediated cleavage of Bid, that in turn, cooperates in the activation of mitochondrial steps in Fas signaling [45].

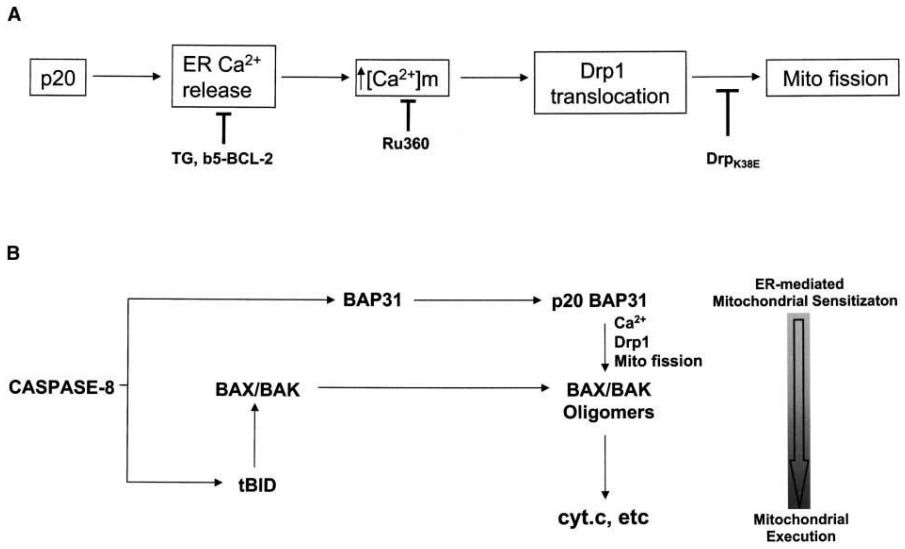

Figure 6: Proposed mode of action of Bap31 fragment p20 [44].

4.3 Recruitment on ER signaling platforms: the role of reticulon 3

In the last years, the subcellular localization of FADD has also been investigated, confirming that, as for caspase-8/procaspase-8 and c-FLIP, besides its cytosolic localization, FADD distributes in the nucleus too [46]. More recently, it has been also described the ability of FADD to localize at the ER upon stimulation of extracellular signals [47], therefore confirming the hypothesis that members of the DRs signaling form intracellular complexes not confined to the plasma membrane. Recruitment of FADD on the ER depends on the interaction between the DD of FADD and the C-terminal domain of members of the reticulon (RTN) family, in particular RTN3 and RTN4B. RTNs are proteins mainly resident in the ER, involved in several functions such as regulation of ER morphology and ER stress response [48]. Treatment with the ER stress inducer tunicamyn, increases this interaction, suggesting that treatments that alter ER equilibrium and cause cell death, can promote the RTN3-dependent recruitment of FADD in ER-bound complexes and the subsequent local activation of caspase-8 and cytochrome *c* release. The dominant-negative of FADD (DN-FADD) impairs the interaction with RTN3, therefore inhibiting caspase-8 activation and Bid cleavage. Conversely no alterations in Bap31 cleavage are reported, indicating that the RTN3/FADD-mediated activation of caspase-8 could be parallel to Bap31 pathway and highlighting the possibility that RTN3 acts as sensor of the ER functionality.

5. THE EMERGING ROLE OF ER-MITOCHONDRIA CROSSTALK IN APOPTOSIS

The importance of subcellular organelles such as mitochondria, ER and the Golgi in the progression of cell death programs, is emerging. As previously described, recent findings suggest that Fas signaling execution depends on complexes localized in ER and mitochondria, or on lipid rafts in the plasma membranes (PM), where components of the DISC are recruited and activated. Intracellular LRs, different in composition from those in the PM have been found both in the ER [49] and mitochondria [50]. In particular, raft-like microdomains localize at the interface between these two organelles, participating in the regulation of ER-mitochondria crosstalk and in the trafficking pathways associated with cell death [51]. ER-mitochondria interactions take place at specific "contact points" between ER membranes and the OMM, known as mitochondria-associated membranes (MAMs) [52]. Very recently, MAMs have been described as LR-like domains [53, 54], enriched in proteins and lipids necessary to physical and functional coupling of ER and mitochondria [55]. In the last years, the role of ER-mitochondria crosstalk in the regulation of apoptosis has gained increasing importance. On the ER several pro- and anti-apoptotic mechanisms converge to mediate cell stress responses. In this regards, calcium storage and handling, which take place in the ER, are particularly significant. For example, proteins of the BCL2 family, that are key components of the intrinsic apoptosis, also exert housekeeping functions in the ER, controlling Ca^{2+} homeostasis, protein folding and apoptosis execution [56] (See below for a thorough description). In particular, Bcl-2, Bax and Bak modulate resting ER Ca^{2+} levels and ER-mitochondria Ca^{2+} exchange, thus influencing the apoptotic response [57, 58]. Moreover, BH3-only proteins of BCL2 family influence the signaling between ER and mitochondria during the unfolded protein response (UPR) associated to the accumulation of unfolded proteins in the ER and the consequent alteration of the ER homeostasis (a condition called ER stress). These findings confirm the importance of ER-to-mitochondria communications in the regulation of Ca^{2+}-exchange and apoptosis. Moreover, they indicate that mediators enriched or recruited at the membranes of these organelles can act promoting the exchange of signals between ER and mitochondria, hence influencing pathways converging in the modulation of cell fate.

6. THE ENDOPLASMIC RETICULUM

The endoplasmic reticulum is a large membranous organelle that spreads throughout the cytoplasm from the nucleus, reaching to the plasma membrane (PM). It was firstly identified in 1945 on electron micrographs [59] and successively divided into two types, smooth and rough ER, based on the presence of bound ribosomes and polysomes [60]. Later on, it was discovered that the nuclear envelope (NE) was another domain of the ER [61]. The ER is a continuous membrane system organized in sheet-like structures, including the nuclear envelope, and in a network of tubules that branch at tripartite junctions to generate a polygonal meshwork, extended throughout the periphery of the cell [62]. It is a unique organelle because of its size, plethora of functions and its ability to interact with virtually all other intracellular organelles. Reflecting these numerous functions, the ER is organized in spatially and functionally distinct subdomains, characterized by a unique set of specialized proteins, some of which characteristically targeted to these domains by intra-ER targeting signals or post-translational modifications (Reviewed in [63]). As already reported, the first subdivision of the ER was originally in smooth or rough ER [64].

The rough ER (RER) is characterized by the presence of bound ribosomes and protein translocation channels (translocons). It is involved in the synthesis and post-translational modification of secretory and membrane proteins. It also contains ER chaperones and oxidoreductases, assisting the folding of newly synthesized proteins (Fig. 7). The nuclear envelope is contiguous with the rough ER but presents bound ribosomes only on the cytosolic face (Fig. 7). It is characterized by specific integral membrane proteins connecting the inner nuclear membrane to chromatin or nuclear lamina and proteins bridging it to the cytoskeleton (Reviewed in [63]). Both RER and nuclear envelope have a sheet-like appearance with low membrane curvature that allows ribosomes and translocons binding [65]. The smooth ER (SER) is devoid of ribosomes [60] and it is shaped as smooth tubules (Fig. 7). It is organized in different specialized subdomains including the ER exit sites (ERES), the plasma membrane-associated ER (PAM) and the ER quality control compartment (ERQC). Specialized enzymes and proteins localize at these functionally distinct subdomains in the smooth ER, thus confirming the existence of intra-ER targeting signals [66]. One of the major functions of the SER is the storage and handling of calcium. In fact, the inositol 1,4,5-trisphosphate receptors (IP_3Rs) and ryanodine receptor calcium channels (RyRs) cluster within the smooth ER [67], forming sub-compartments devoted to Ca^{2+} homeostasis [68] and

mobilization toward other ER-interacting organelles such as mitochondria and the plasma membrane (Fig. 7).

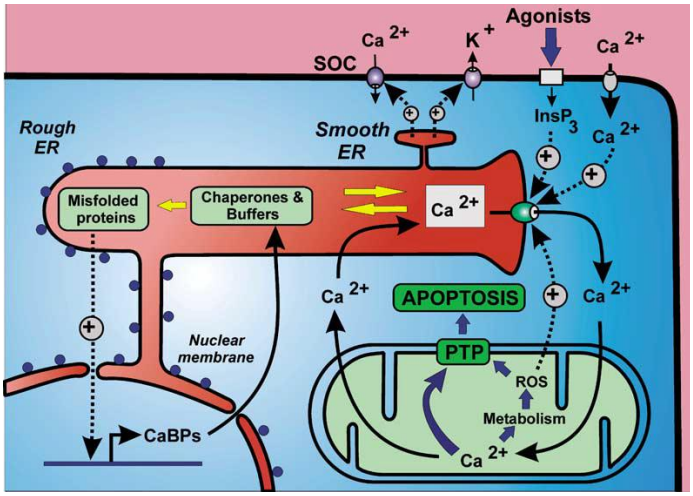

Figure 7: Structural and functional heterogeneity of the ER [69].

6.1 Mechanisms regulating ER dynamics

Mechanisms of organelle shaping exist and regulate ER dynamics, promoting the formation of sheet-like structures or interconnected tubules, which share a single and continuous lumen, but accommodate distinct physiological functions, hence guaranteeing the maintenance of the multifunctionality of this organelle. In particular, flattened sacks typical of cisternal ER are better suited for ribosome binding and association of translocation machinery, therefore characterizing the RER. Conversely, tubular ER, that mainly features the SER, presents multiple regions of high membrane curvature, that better accommodate rapid calcium signaling and membrane traffic (Reviewed in [70]). Moreover, the ER structure is constantly remodeled. This dynamic behavior reflects its ability to adapt to constantly changing cellular requirements relying on rapid ER restructuring and on partitioning of particular proteins. Even though mechanisms regulating ER dynamics are still not fully understood, great advances have been made in the last years, identifying some of the proteins involved in ER membrane biogenesis and remodeling. Among mechanisms responsible for organelle shaping, a fundamental role has been attributed to the so-called ER-shaping proteins. Members of the RTN (reticulon), DP1 (Deleted in Polyposis Locus Protein 1) and atlastin (ATL) families

regulate tubule formation and fusion. By contrast, morphology of cisternae is modulated by the sheet-enriched proteins 63-kDa cytoskeleton-linking membrane protein (CLIMP63), p180 and kinectin.

6.2 Shaping the reticular ER: the role of RTN/DP1

Proteins firstly identified as necessary and sufficient to ER biogenesis and tubulation belonged to the RTN and DP1 families [71]. These proteins are ubiquitously expressed and mainly localize in the ER membranes. In particular, members of the two families have been shown to be highly enriched in ER tubules, whereas they are excluded from cisternae and nuclear envelope, even when overexpressed. Both topology and oligomerization features of these proteins have been suggest to contribute to their localization and ability in shaping the ER. In fact, RTN/DP1 are both characterized by the presence at their C-terminal domain of two long, hydrophobic domains (RDH domain), separated by a hydrophilic region. Each transmembrane domain form a hairpin in the lipid bilayer, that is necessary to anchor RTN/DP1. Conversely, the N- and the C-terminal and the soluble region remain exposed to the ER lumen (Fig. 8) [72]. Deletion of RTN and DP1 genes in yeast and mammalian cells results in a great loss in the ER tubules, which convert to a sheet-like appearance [71]. Two cooperative mechanisms have been proposed to act in shaping ER tubules. First of all, insertion of the hairpin structure in ER bilayer forms a wedge preferentially in the upper part of the outer monolayer, causing a local high curvature in ER tubules. Furthermore, oligomerization in the lipid bilayer allows the formation of arc-like structures around the membranes, consequently forcing them into a tubular shape. Oligomers disassembly is ATP dependent, suggesting that they are continuously formed and disassembled, without impairing freely diffusion of ER luminal proteins [73]. These findings together suggest that both RTNs and DP1 are ‘‘morphogenic’’ proteins that are necessary to form and maintain ER peripheral tubules, by curvature-inducing and scaffolding mechanisms.

6.3 Branching the ER: the role of Atlastins

After the tubules are formed by the curvature-inducing activity of RTN/DP1, tubules are connected each other, to form the typical meshwork of three-way junctions. The atlastins proteins are involved in the homotypic fusion of adjacent ER tubules [74]. The ATLs are integral membrane GTPases belonging to the dynamin family, mainly localized at the tubular ER. Two C-terminal TM domains form a hairpin in the membranes, mediating both the localization of ATLs and their interaction with RTN/DP1. Indeed, oligomers of ATLs associate to RTNs/DP1 at high-curvature regions, interacting from apposing tubules and tethering adjacent membranes. Upon coordinated, GTP-dependent, conformational changes, ATLs pull the two membranes in close proximity, and insert their amphipathic C-terminal into the lipid bilayer of adjacent tubules, destabilizing them and facilitating their fusion [74, 75]. Depletion of ATLs in mammalian cells results in unbranched ER tubules, whereas their overexpression causes the aberrant proliferation of sheet-like cisternae, probably due to the excessive fusion of ER membranes [72].

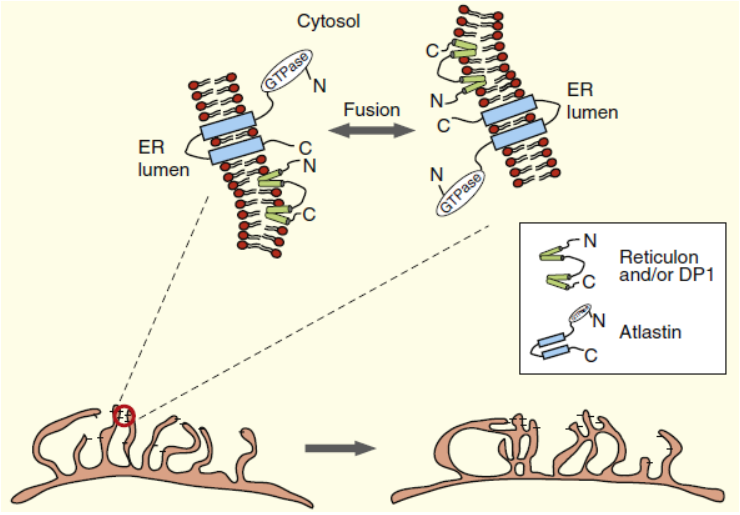

Figure 8: Molecular model for the generation of ER tubules [72].

6.4 Shaping the cisternal ER: the role of coiled-coil proteins

Morphological differences among ER domains are partially related to variations in membrane curvature that enable regulation of domains shape, despite maintaining them physically continuous. The peripheral ER cisternae in most species are similar in luminal thickness to the tubules, but occur as flat sheet-like structure, curved only at the edge, with a degree of curvature similar to ER tubules. It has been demonstrated that curvature-stabilizing proteins RTN/DP1 are sufficient to keep the two membranes of a sheet closely apposed, by a wedging and scaffolding mechanism, as for ER tubules [76]. However, additional factors contribute to stabilize ER sheets. Among these, it has been determined a role for sheet-enriched, coiled-coil membrane proteins such as CLIMP63, p180 and kinectin (Fig. 9). CLIMP63, which is the best characterized, serves as a luminal spacer, optimizing the size of the luminal space of peripheral ER cisternae. In fact, interacting coiled-coil domains of different CLIMP63 molecules, which extend from apposing membranes of a sheet, control cisternal width [77]. By contrast, p180 and kinectin, whose coiled-coil domains are cytosolic, interact with cytoskeletal components, anchoring ER sheets to microtubules and contributing to flatten their surface. At the same time, localizing at ER sheets, coiled-coil proteins generate an "osmotic pressure" that counteracts the shrinkage of cisternae due to the high curvature at the edge. Accordingly, coiled-coil proteins are not essential for sheet formation per se, whereas RTN/DP1 provide the basic mechanism by which both sheets and tubules are generated [76]. Consequently, the cell-type-specific ratio of sheets to tubule in the peripheral ER depends on abundance of curvature-inducing proteins and the the relative amount of RTN/DP1 and coiled-coil proteins. In agreement, increased expression of RTNs reduces the number of ER sheets, whereas its reduction or the overexpression of CLIMP63 cause sheets proliferation [76].

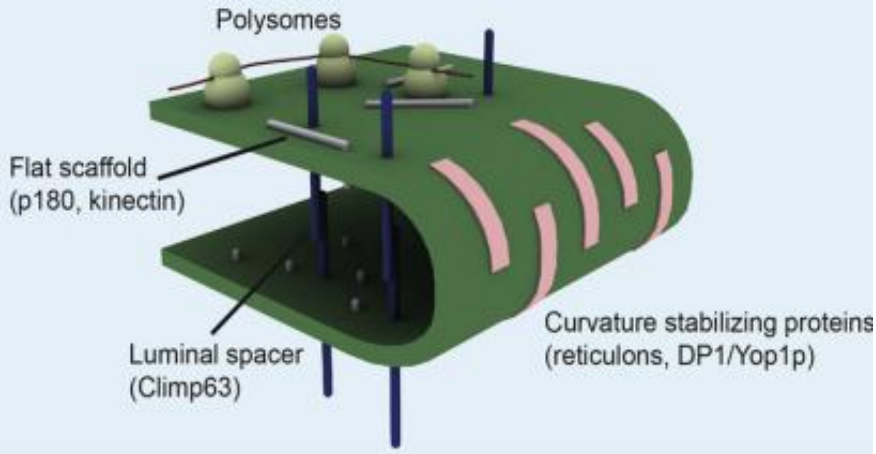

Figure 9: Molecular model for the generation of cisternal ER [77].

6.5 Other factors shaping the ER

Additionally to RTN/DP1 and sheet-enriched proteins, also membrane-bound polysomes contribute to ER-sheets shape maintenance. Polysomes enrichment on flat cisternae (Fig. 9) participates in concentrating sheet-localized proteins such as translocons and their disassembly therefore causes an equally distribution of these proteins between tubules and sheets and contribute to reduce the amount of peripheral cisternae, similarly to depletion of the sheet-promoting proteins. At the same time, coiled-coil proteins, favoring the enlargement of cisternal surfaces, allow more polysomes to bind and distribute, hence stabilizing the RER [76].Other mechanisms shaping and stabilizing the ER include interactions with cytoskeleton components or other organelles, such as mitochondria. In animal cells, the peripheral ER is in close contact with cytoskeleton and tracks along microtubules (MTs) to spread throughout the cytoplasm (Reviewed in [65]). Despite microtubules are not required for tubule formation, they influence the appearance of ER, as their disruption with the drug nocodazole causes the collapse of the reticular ER and its retraction toward the nucleus. Confirming the role of cytoskeleton in the regulation of ER morphology, it has also been reported that sheet-promoting proteins CLIMP63, p180 and kinectin mediate linking and sliding of the ER along microtubules, even though the link between coiled-coil proteins and microtubules in the regulation of ER morphology remains still unclear.

6.6 Multidomain organization of the ER

As previously described, segregation of the ER into only SER and RER remains simplistic because of the existence of multiple specialized subdomains. In the last years, subdomains involved in the functional and physical coupling of the ER to almost all other subcellular organelles (Fig. 10) have been largely investigated. Moreover, interactions with these organelles have been related to the stabilization of ER network, therefore regulating organelle shaping and modulating cellular responses.

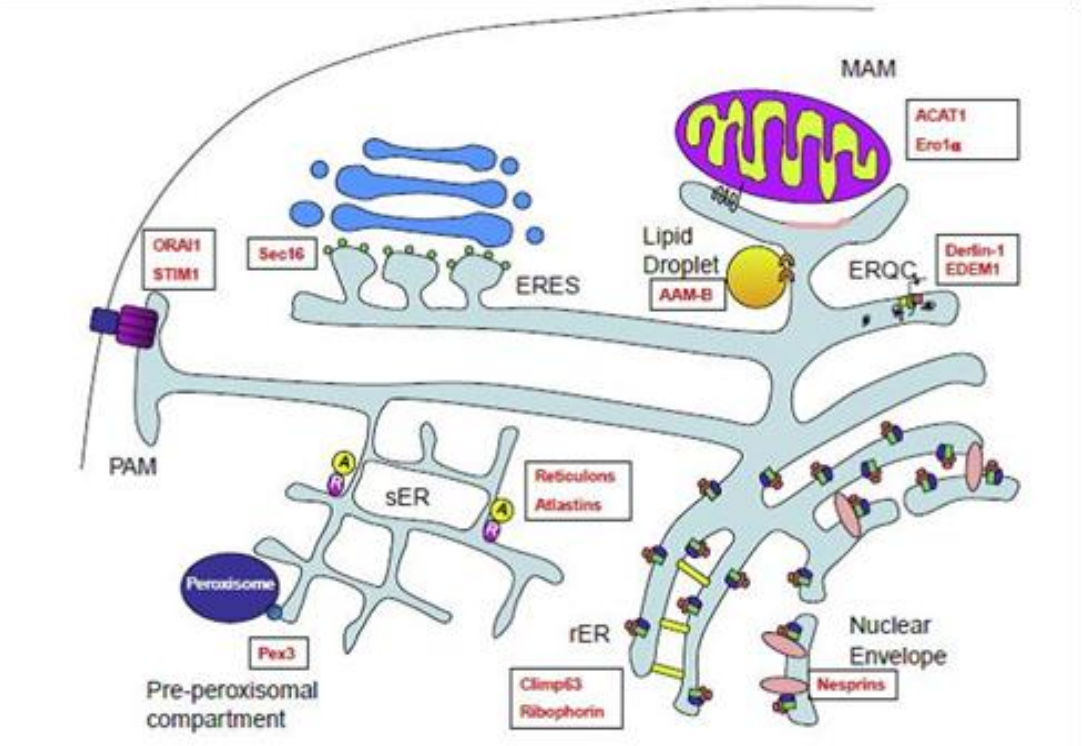

Figure 10: ER subdomains and specific markers [63].

6.7 The plasma membrane-associated ER

The ER extensively contacts the plasma membrane (PM), being associated to the 20-45% of the cytosolic face of the PM, at least in yeast [78]. In yeast and mammalian cells ER-PM distance is estimated at a mean spacing of 33nm, therefore excluding ribosomes from this interface [78]. These contact sites are important for the regulation of phosphatidyl inositol metabolism and constitute a major site of synthesis for phosphatidylserine [79]. Moreover, in mammalian cells, the PAM plays a crucial role in calcium homeostasis. In fact, when ER Ca^{2+} stores are depleted, the ER-localized stromal interaction molecule 1 (STIM1) and the PM protein calcium release-activated calcium channel protein 1 (Orai1) interact, promoting Ca^{2+} influx into the ER [80]. ER dynamics and proteins modulating it are also important to both coordinate activities of interacting organelles and to regulate Ca^{2+}-homeostasis. Indeed, a massive ER remodeling, similar to that induced by RTN/DP1 ablation, has been observed upon Ca^{2+} depletion: enlargement of ER cisternae and their association to PM are in fact necessary to Ca^{2+} funneling to the ER [78, 81].

6.8 Other organelles contacting the ER

It is now clear that the ER contacts several organelles and can also be involved in organelle generation. It has been demonstrated that ER-GOLGI functional interactions take place in the secretory pathway. Moreover, very close and stable contacts have been identified between the *trans*-ER regions and *trans*-cisternal Golgi to sustain a non vesicular-trafficking that transports lipids from the ER to the Golgi, maintaining the characteristic composition of the latter [82].

The ER also contacts endosomes and late-endosomes, both coordinating the movements of early endosomes with the ER dynamics and regulating the intracellular distribution of late endosomes (Reviewed in [70]).

Additionally, the smooth ER, in particular the pre-peroxisomal compartment, is involved in generation of peroxisome[83], which mediate the degradation of long chain fatty acids [84], and close contacts between the two membranes have also been found (Reviewed in [63]).

7. THE MITOCHONDRIA-ASSOCIATED MEMBRANEs (MAMs)

Subcellular organelles modulate signaling cascades by compartmentalizing second messengers such as calcium and therefore modulate the strength, the duration and the localization of signals controlling cell activities. In fact, it is not surprisingly that organelles interact each other and that their reciprocal positions in the cytosol are organized to allow efficient functional coupling. The interaction between the endoplasmic reticulum and mitochondria has been extensively investigated in the last years because of the important implications on cell metabolism, apoptosis and calcium signaling that these two organelles exert. First evidences of a close contact between ER membranes and the mitochondrial outer membrane (OMM) date back to the late Fifties [85] and were successively confirmed by several groups. Following studies based in subcellular fractionation protocols led to the isolation of ER membranes co-purifying with mitochondria [86] that were successively named mitochondria-associated membrane (MAM) by Jean Vance, who identified for the first time these contact sites as implicated in the exchange of phospholipids between the two organelles [52]. More recently, it has been determined that physical, proteinaceous bridges, of 10-25nm in length, link ER and mitochondria [87], and that 20% of the mitochondrial surface is in contact with the ER [88]. Functional coupling of the organelles at the MAM was further confirmed by the finding that at the contact points calcium transfer from the ER to mitochondria occurred in a "quasi-synaptic" manner [89], regulating cell metabolism and apoptosis onset (Reviewed in [90, 91]).

Organization of ER membranes in functionally distinct subdomains suggests that mechanisms of intra-organelle protein sorting must exist. Known targeting signals direct proteins to the ER or mitochondria. By contrast, signals directing proteins specifically to the MAMs have not been clearly identified yet. It has been hypothesized that varying degrees of membrane curvature could accommodate different proteins such as for the RTNs or CLIMP63 [76]. Otherwise, post-translational modifications such as phosphorylation and palmitoylation can alter targeting sequences, influencing protein distribution. The transmembrane, ER-resident chaperone calnexin (CNX) localizes also at MAMs [92] and its distribution partially depends on the phopsphorylation within an acidic cluster recognized by the MAM-localized protein phosphofurin acidic cluster sorting protein 2 (PACS2) [93], which therefore regulates the amount of CNX at the MAMs or RER [92]. Additionally, palmitoylation of CNX itself and of other MAM-proteins such as heme oxigenase-1 and disulphide isomerases TMX and TMX2 contributes to their targeting. These findings suggest that palmitoylation of cytosolically

exposed cysteines could be a new sorting signal for ER membrane proteins [94]. In comparison to the relatively stable association of CNX to the MAMs, the localization of another MAM-enriched protein, the ER oxidoreductase 1α (Ero1α), is highly susceptible to the redox state and oxygen supply. Ero1α mediates the re-oxidation of the ER disulfide isomerase PDI, by its flavin adenine dinucleotide (FAD) prosthetic group that transfers electrons from cysteines to molecular oxygen. The vicinity of PDI/Ero1α complexes to mitochondria would result in the higher availability of mitochondrial ATP and FAD, necessary to the efficient oxidative protein folding. Hypoxia leads to the rapid depletion of Ero1α from the MAM suggesting that not only post-translational modifications, but also changes in oxidizing conditions could alter mechanisms of protein retention into the ER, moving ER proteins toward or away from the site where their activity is required [95]. Similarly, MAMs lipid composition influences the anchoring of the sigma-1 receptor at these sites, where this Ca^{2+}-handling protein promotes the fine-tuning of Ca^{2+} exchanges with mitochondria [53, 93].

As previously reported, in the last years different groups identified intra-organelles lipid rafts-like domains [49, 50]. More recently, technical improvements in subfractionation techniques allow to discriminate between PM-derived and intracellular LPs, demonstrating that MAMs have the characteristics of a lipid raft and are able to recruit and orientate different signaling proteins needed for the ER-mitochondrial crosstalk and tethering [53, 54]. Alterations in liquid-ordered structure or protein composition of ER membrane at ER-mitochondria interface could thus influence both the physical and functional coupling of the organelles. Moreover, the fact that the MAMs are lipid rafts-like domains could explain discording data reporting the presence of some proteins, such as presenilins and γ-secretase, at both PM and ER/mitochondria [96, 97].

7.1 ER-Mitochondria tethering

Proteinaceous bridges at the contact sites between ER and mitochondria modulate the physical tethering of the two membranes. Both organelles are continuously and concertedly remodeled by fusion and fission events. Therefore, it's not surprisingly that proteins required to membrane remodeling, are also involved in ER-mitochondria juxtaposition. To date, a function in organelle tethering has been demonstrated for the mitochondrial-shaping proteins mitofusin (MFN) 1 and 2, and dynamin-related protein (DRP1). The first direct, physical ER-mitochondria linkage to be discovered was MFN2 [98]. MFN2 was found to localize both in mitochondria and MAMs and to a lower extent in the ER. Mitochondrial MFN2 it is known to regulate mitochondrial fusion and morphology. Conversely, at MAMs, MFN2 regulates ER shape and tethering to mitochondria by engaging homo- and hetero-complexes respectively with MFN2 and MFN1 on the OMM. Both mitochondria [99] and ER [65] interact with microtubules and other cytoskeleton elements, that could act both as scaffolds to stabilize the interactions between the organelles and to contribute to the coordinated remodeling of ER and mitochondria. Accordingly, the cytoskeleton-binding protein Trichoplein/mitostatin (TpMs), previously identified as loosely attached to the OMM, has also been found at the ER-mitochondria interface, where it regulates mitochondrial morphology and juxtaposition to the ER in a MFN2-dependent manner [100]. Another direct, physical linker between the two organelles has been revealed in yeast, by a synthetic biology screen, but its homolog in mammal cell has not been found yet. This complex, named the ER-mitochondria encounter structure (ERMES), includes proteins localized in the OMM or at ER surface and at their interface [101]. Recently the ERMES complex has been related also to the efficient lipid exchange in yeast, confirming the role of MAMs in lipid metabolism and exchange, and thus suggesting that protein complexes regulating the structural tethering could also be necessary to a functional modulation of MAMs activities [102]. Other MAM-resident proteins such as DRP1 and PACS2 have been implicated in the regulation of ER-mitochondria tethering, by modulation of organelle integrity even though they do not take directly part in the physical anchoring of the two membranes [90]. Alterations in mitochondrial morphology have been associated to altered juxtaposition of the two compartments [98]. The relation between organelle morphology and tethering was further confirmed by investigating the role of the MAM-protein PACS2. The multifunctional sorting protein PACS2 controls organelles apposition because its ablation causes mitochondrial fragmentation and uncouples the

mitochondria-ER axis. PACS2 depletion in fact induces the caspase-dependent cleavage of the ER- and MAM-localized Bap31, which in turn promotes mitochondrial fission, through the recruitment of the dynamin-related protein 1 (Drp1) [103]. Moreover, PACS2-depleted cells are less sensitive to apoptotic stimuli based on the exchange of calcium and signals between ER and mitochondria [103]. Mitochondria-associated membranes are also enriched with molecular chaperones such as calnexin and Bip/Grp78, involved in both regulation of protein folding and Ca^{2+}-handling and exchange with mitochondria. Among chaperones, an indirect role in the regulation of the distance between ER and mitochondria has been revealed for the chaperone glucose-related protein 75 (Grp75) [104]. Grp75 is a mitochondrial protein, that in the OMM forms a complex spanning the membranes of the two organelles with the voltage-dependent anion channel (VDAC) on the mitochondrial side and the IP_3R on the ER membrane. In this complex, Grp78 indirectly regulates tethering of the two membranes acting as a scaffold to promote the physical coupling of VDAC and IP_3R and maximize Ca^{2+}-exchange at the ER-mitochondria interface [104]. Concluding, even though great advances have been made in the identification of proteins and complexes regulating the physical tether or the functional crosstalk between ER and mitochondria (Fig. 11), several other possible mechanisms remain still unknown and need to be addressed in the future.

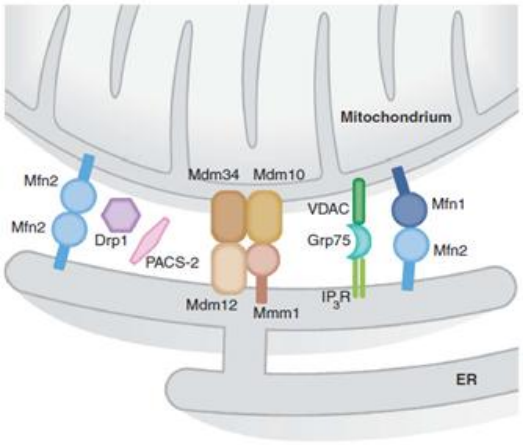

Figure 11: Tethers between ER and mitochondria [90].

7.2 Functional crosstalk: lipid synthesis and transport

MAMs are characterized by a specialized proteome that determines their structure and functions. As described before, this subdomain of the ER was primarily identified for its involvement in the storage, exchange and metabolism of different classes of lipids. Proteins firstly found in this localization in fact included enzymes associated to lipid synthesis, such as the fatty acid CoA ligase 4 (FACL4), used as a MAM marker; phosphatidylserine synthase 1 and 2 (PSS1, PSS2); the acyl-coenzyme A:cholesterol acyltransferase-1 (ACAT1); the acyl-CoA:diacylglycerol acyltransferase 2 (DGAT2) and the phosphatidylethanolamine methyltransferase 2 (PEMT2) (Reviewed in [105]). Moreover, enrichment in lipids and synthesizing enzymes contribute to explain the lipid-rafts like properties of these ER subdomains. Synthesis of phosphatidylcholine (PC), that occurs at the MAMs, represents the most evident example of the ability of the two organelles to exchange lipids. Phosphatidylserine (PS), precursor of PC, is synthesized at MAMs, where PSS1 and PSS2 activity is focused. PS is then converted to phosphatidylethanolamine (PE) on mitochondria, suggesting that a direct transfer from the ER toward mitochondria is necessary. Finally, PE is shuttled back to the ER, at the MAMs, where it is further converted into PC by PEMT2 (Reviewed in [90, 105]). These, and other findings, together suggest that the interface between ER and mitochondria has a primarily role in lipids metabolism and exchange.

7.3 Functional crosstalk: calcium signaling regulation

Among proteins enriched at the interface between ER and mitochondria, a large group is represented by proteins involved in Ca^{2+}-handling, comprising channels deputed to the Ca^{2+} release/uptake and molecular chaperones (Fig. 12). Cytosolic calcium concentration ($[Ca^{2+}]_c$) in resting conditions is maintained around 100nM, a value significantly lower than in the extracellular space (1mM). Low permeability and calcium pumps at the PM guarantee these ranges of values. However, rapid cytosolic Ca^{2+} transients occur through Ca^{2+} mobilization from internal stores, or inducing the entry from the extracellular space, reaching values around 1-2µM. The ER represents the main intracellular calcium store and releases calcium through different receptors. The main route inducing calcium release from the ER involves the IP_3 Receptors (IP_3Rs), which bind on their cytosolic side the inositol-1,4,5-triphosphate (IP_3), successively opening their transmembrane domain and forming a Ca^{2+} channel (Reviewed in [106]). Other receptors stimulating ER calcium release are the Ryanodine Receptors (RyR), which are activated by the alchaloid ryanodine and by Ca^{2+} itself (Reviewed in [106]). Intracellular Ca^{2+} concentration is tightly regulated because of the several implications of this second messenger in cell functions, and several mechanisms assure the maintenance of low Ca^{2+} levels (Reviewed in [107]). Among these, a growing attention has been addressed to the role of mitochondria as buffering organelles. Physiological, Ca^{2+}-mobilizing stimuli elicit a $[Ca^{2+}]_c$ rise theoretically insufficient to induce mitochondrial calcium uptake, because of the low affinity of mitochondrial Ca^{2+} transporters, varying between 10^{-6} and 10^{-4} M. Paradoxically, upon ER Ca^{2+}-release, mitochondria could rapidly accumulate calcium down the electrochemical gradient of their membranes (-180mV, negative inside). This apparent contradiction between the prompt response of these organelles and the low affinity of their transporters, led to the formulation of the "hotspot hypothesis" [91]. In response to different stimuli, high-Ca^{2+}, transient microdomains are formed at the interface between ER and mitochondria, where ER releasing channels and mitochondrial transporters are enriched. The close apposition between the two organelles allows the formation of subcellular domains where the $[Ca^{2+}]_c$ largely exceed the bulk of cytosolic values, therefore meeting the low affinity of mitochondrial transporters and inducing Ca^{2+} uptake [108]. MAMs therefore represent a privileged region regulating ER-mitochondria Ca^{2+}-exchange, as also confirmed by the ablation of key proteins localized at these contact sites. In fact, cells depleted for these key regulating factors, show altered regulation of the

organelle tethering and functional crosstalk, both impacting on the modulation of cell metabolism and cell death responses stimulating ER calcium release. To date, a clear relation between variations in ER-mitochondria tethering and calcium signaling has been reported as a consequence of MFN2 ablation [98]. Also the ablation of MAM-localized, Ca^{2+}-regulating proteins affects the calcium exchange. Among these (see Figure 14), the Sigma-1 Receptor, PACS2 and the complex including IP3R/Grp75/VDAC, influence calcium signaling at the mitochondria-associated membranes, by stabilizing or modulating the activity of involved receptors [108].

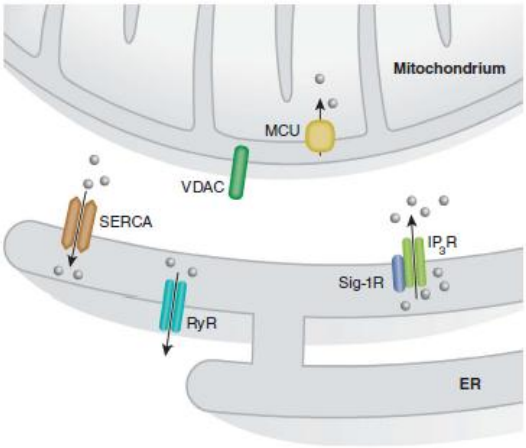

Figure 12: Ca^{2+}-handling complexes and apoptosis-regulator factors at the MAMs [90].

7.4 Functional crosstalk: modulation of cell death responses

Transient variations in $[Ca^{2+}]_c$ trigger several cellular functions including cell proliferation, cell metabolism and regulation of apoptotic responses. In physiological conditions, there is a continuous transfer of calcium from the ER to mitochondria necessary to the Ca^{2+}-dependent activity of the mitochondrial enzymes of the tricarboxylic acid cycle. Ca^{2+} supply to mitochondria is hence indispensable to ATP production and cellular bioenergetics and survival [106] (Fig. 13). Upon several pro-apoptotic insults such as H_2O_2 and ER stress, an increased flux of Ca^{2+} to the mitochondria is observed, impacting on cell survival (Fig. 13). In fact, calcium overload impairs mitochondrial functions, by increasing the membrane permeability through the opening of the "permeability transition pore" and the release of cytochrome *c* and other pro-apoptotic proteins (Reviewed in [108]). In this view, the spatial proximity mediated by proteins and complexes at the MAMs is necessary to the efficient transfer of calcium and apoptotic signals between the two organelles. Similarly, conditions that alter ER functioning, including variations in the ER Ca^{2+} concentration ($[Ca^{2+}]_{ER}$) and aggregation of unfolded proteins (the so-called ER stress), can modulate the apoptotic response. Proteins endogenously localized or recruited upon cell death induction at the ER-mitochondria interface, can modulate the effective $[Ca^{2+}]_{ER}$ released, thus impacting on the transmission of cell death signals to mitochondria. As previously described, sigma-1, and PACS2, at the MAMs, couple specific Ca^{2+}-channel, partially stabilizing them and regulating Ca^{2+}-dependent signaling and apoptosis. Similarly several important apoptosis regulators have been described as crucial modulator of Ca^{2+}-mediated apoptosis. Some BCL-2 family members, besides their localization in mitochondria and cytosol, reside also in the ER. It has been demonstrated that these proteins represent key factors in tuning Ca^{2+}-release and $[Ca^{2+}]_{ER}$, thus influencing apoptosis induction (Fig. 13). The anti-apoptotic protein Bcl-2 was the first identified as regulator of Ca^{2+}-homeostasis [57]; later on also Bcl-X_L was found to act in a similar way. Depending on their recruitment on the ER surface, overexpression of both proteins decreases resting $[Ca^{2+}]_{ER}$ through the destabilization of SERCA pumps on the ER, thus enhancing Ca^{2+}-emptying (Reviewed in [109]). Moreover, Blc-2 could also interact with the IP_3R and inhibit IP_3-mediated Ca^{2+}-mobilization upon apoptosis induction, leading to a reduced Ca^{2+}-release in the cytosol and a decreased mitochondrial Ca^{2+}-entry, therefore limiting the sensitivity to apoptotic stimuli ([110]).

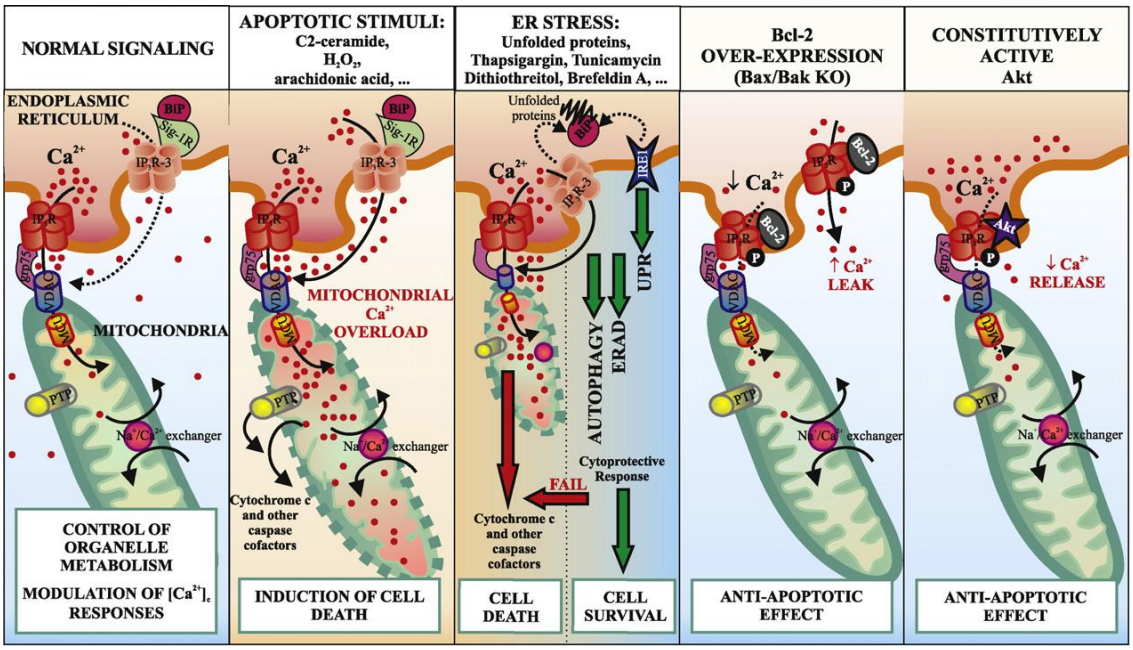

Figure 13. ER-mitochondria Ca^{2+}-exchange in physiology and apoptosis [91].

Similarly, also the ER-localized anti-apoptotic proteins Bax and Bak are implicated in Ca^{2+} homeostasis, through the elevation of the resting $[Ca^{2+}]_{ER}$ [58]. Indeed, cell depleted for both these proteins were more resistant than WT to apoptosis due to the reduction in ER releasable Ca^{2+}. Together these findings suggested that pro- and anti-apoptotic factors, besides their role at the mitochondria, could also regulate the apoptotic response localizing at the ER. In this localization, they alter the ER Ca^{2+}-content, hence influencing both calcium exchange and functional crosstalk between ER and mitochondria. Also cytosolic factors could be recruited at the ER-mitochondria interface to regulate the activity of Ca^{2+}-channels (Fig. 13). Among these, it has been demonstrated that the complex including the anti-apoptotic AKT/PKB kinase [111], the tumor-suppressor PML (promyelocytic leukemia protein) and the phosphatase PP2a (protein phosphatase 2a) [112], regulates the phosphorylation status and consequently the activity of IP_3R_3. Active AKT, in response to survival signals, distributes on MAMs and hyperphosphorylates the IP_3R_3, inactivating it and reducing ER calcium release and apoptosis induction. Conversely, PML, interacting with AKT and the phosphatase PP2a, recruits PP2a which in turn reduces the amount of phosphorylated and active AKT, therefore restoring activation of IP3Rs and sensitivity to apoptosis. Another condition that induces Ca^{2+}-release from the ER and the Ca^{2+}-dependent ER-mitochondria crosstalk is the so-called ER stress. Conditions saturating the folding capacity of the ER and thus causing the accumulation of unfolded proteins are

referred to as ER stress (Reviewed in [113]). Several physiological stimuli, as well as pharmacological treatments or depletion of ER Ca^{2+} stores, induce ER stress. Different feedback mechanisms control the efficiency and fidelity of protein folding, activating a series of adaptive signaling pathways when ER homeostasis is altered. These adaptive responses are collectively defined the unfolded proteins response (UPR), which activates an ER-to-nucleus signaling pathway leading to the attenuation of global translation, although synthesis of chaperones is conversely increased to improve ER folding capacity (Reviewed in [114]). Three converging pathways are activated upon ER stress and they are mediated by the three sensors IRE1α (inositol requiring kinase α), ATF6 (activating transcription factor 6) and PERK (protein kinase-like ER kinase) (Fig.14). These signaling pathways also increase cell proteolytic ability, through the activation of autophagy or retrotranslocation of unfolded polypetides into the cytosol to proteasomal degradation (Reviewed in [113]). However, these cytoprotective responses fail when the ER stress persist, therefore switching to cell death induction. The induction of an ER stress-dependent apoptosis has a mandatory mitochondrial phase which is activated by the transfer of Ca^{2+} from the ER to mitochondria and consequent mitochondrial Ca^{2+}-overload (Fig. 13). Efficient ER-mitochondrial coupling and Ca^{2+}- exchange through the IP_3R-VDAC complex are therefore essential to apoptosis induction. In agreement, PML depleted cells, whose IP_3Rs are inactive due to the increased activity of AKT, show increased resistance upon treatment with the ER stressors thapsigargin and tunicamycin, and to calcium-dependent apoptosis induced by H_2O_2 [112]. Moreover, the role of ER-to-mitochondria communication in ER stress-mediated cell death has been further corroborated by the findings that BH3-only, pro-apoptotic members of the BCL-2 family, which are retrieved in the ER, can activate a particular branch of the ER stress signaling pathway mediated by IRE1α, which in turn promotes the Ca^{2+}-dependent sustained JNK activation and apoptosis (Fig. 14) [56, 115].

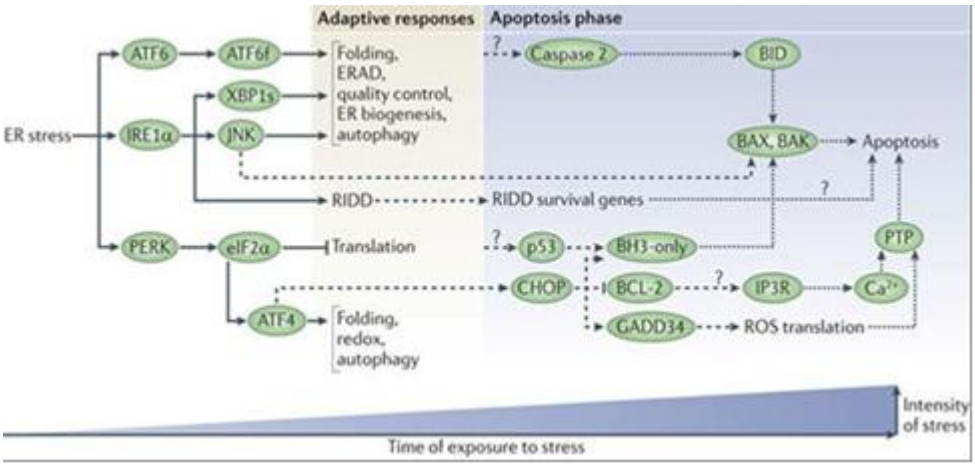

Figure 14: Cell fate decisions under ER stress [114]

AIM OF THE PROJECT

Caspase-8 and FADD are components of the DR-signaling. Besides their localization in the cytosol or their recruitment in lipid-rafts at the plasma membrane upon apoptosis induction, in the last years, several groups have observed the distribution of procaspase-8/caspase-8 and FADD in local complexes associated to mitochondria and ER, organelles critically involved in regulation of cell death. Existence of these complexes and cleavage of local substrates could therefore explain the described ability of these proteins to modulate several apoptosis-independent pathways. c-FLIP is the best characterized caspase-8 inhibitor. In our group, in a c-FLIP overexpressing transgenic mouse model, this protein has also been observed in association with mitochondria (unpublished data). Therefore, as first aim of the present study, in collaboration with Luca Scorrano (Venetian Institute of Molecular Medicine), we investigated the subcellular localization of endogenous c-FLIP. Surprisingly, we found that c-$FLIP_L$ was retrieved at the ER and MAMs, an ER subdomain physically and functionally coupled to mitochondria. This novel and unexpected localization prompted us to investigate the functional involvement of c-$FLIP_L$ in regulation of organelles morphology and ER-mitochondria crosstalk, using as experimental models c-$FLIP^{-/-}$ and WT MEFs. As second aim of this study, we therefore evaluated ER and mitochondria integrity in these cell lines by both morphological and biochemical analysis. Moreover, since the ablation of proteins enriched at MAMs is often associated to alterations in the ER-mitochondria distance and consequently in the exchange of Ca^{2+} and pro-apoptotic signals between these two organelles, as third aim of this project we investigated c-FLIP role in the regulation of both ER-mitochondria physical tethering and functional crosstalk. To this aim, we explored Ca^{2+} signaling and apoptotic responses to ER stress, in WT and c-FLIP depleted cells.

RESULTS

1. c-FLIP$_L$ localizes at the ER and MAMs

Components of the extrinsic apoptosis machinery such as FADD and procaspase-8/caspase-8 have been primarily described as cytosolic or recruited in complexes at the plasma membranes. In the last years however, these proteins have also been found associated to nucleus, mitochondria and ER as described in the introduction section. Similarly c-FLIP, the principal caspase-8 inhibitor has been described as mainly cytosolic and more recently as nuclear. To better determine the subcellular localization of endogenous c-FLIP, we investigated its distribution in isolated purified fractions from mouse liver (Figure 1A-B). We firstly evaluated cross-contaminations probing each fraction for an organelle specific marker (Figure 1A). Under our experimental conditions, purified mitochondria showed as expected an enrichment in the mitochondrial translocase of the outer membrane (TOM20), which was absent in fractions derived from ER, MAMs and cytosol. MAMs were identified by the specific marker fatty acid-CoA ligase 4 (FACL-4). Calnexin (CNX), as expected, was enriched in the light membranes (ER+LM) fraction, that mainly contains membranes from ER, and MAMs [94]. Finally, the cytosolic marker Lactate dehydrogenase (LDH) was only present in the correspondent fraction from cytosol. As shown in Figure 1B, we identified c-FLIP$_L$ in the ER+LM and MAMs fractions, besides the well documented localization in the cytosol, whereas it was not detectable in purified mitochondria. Moreover, cleavage fragments of this protein were mainly found in the cytosol. By contrast, we didn't clearly identify the localization of c-FLIP$_{S,R}$ in any fraction, even though, according to our results and data from literature, these short isoforms seemed to mainly reside in the cytosol. The novel subcellular localization for c-FLIP$_L$ prompted us to investigate its functional role in the regulation of ER-mitochondria axis. To this aim, we used immortalized mouse embryonic fibroblasts (MEFs) derived from the lethal c-FLIP knockout mouse model [25] and their WT counterparts. To confirm whether c-FLIP was similarly distributed in our model, WT MEFs were fractionated. Purified fractions from cell culture are usually less easily obtained, because of technical difficulties. For this reason we investigated c-FLIP$_L$ localization only in ER+LM, cytosol and crude mitochondria. c-FLIP$_L$ distribution was confirmed in ER and cytosol, and it was also identified in crude mitochondrial fraction that contains the ER- and MAM-localized

CNX (Figure 1C). Subcellular distribution of c-FLIP in the ER and ER-mitochondria contanct points of WT cells was also confirmed by immunofluorescence and confocal analysis. In Figure 1D representative confocal images of WT MEFs were shown. Mitochondria were revealed using the specific pDsRed2-mito plasmid, whereas antibodies against c-FLIP and the ER marker calreticulin (CRT) were used. In the upper panel, we reported the co-localization between ER and mitochondria. Yellow discrete areas represented overlapping regions of the two organelles. Similarly to CRT, c-FLIP displayed a patchy staining in discrete areas of mitochondria (middle panel), therefore confirming its localization at the ER-mitochondria contact points. Conversely, a wider co-localization between the reticular CRT and c-FLIP was shown in the lower panel. Taken together, our findings suggest a novel and unexpected localization for c-FLIP$_L$ at the ER and MAMs. Furthermore, the localization of DISC components at the ER-mitochondria interface indicate that these regions could be involved in the regulation of both apoptotic and non-apoptotic death receptors-mediated cellular functions.

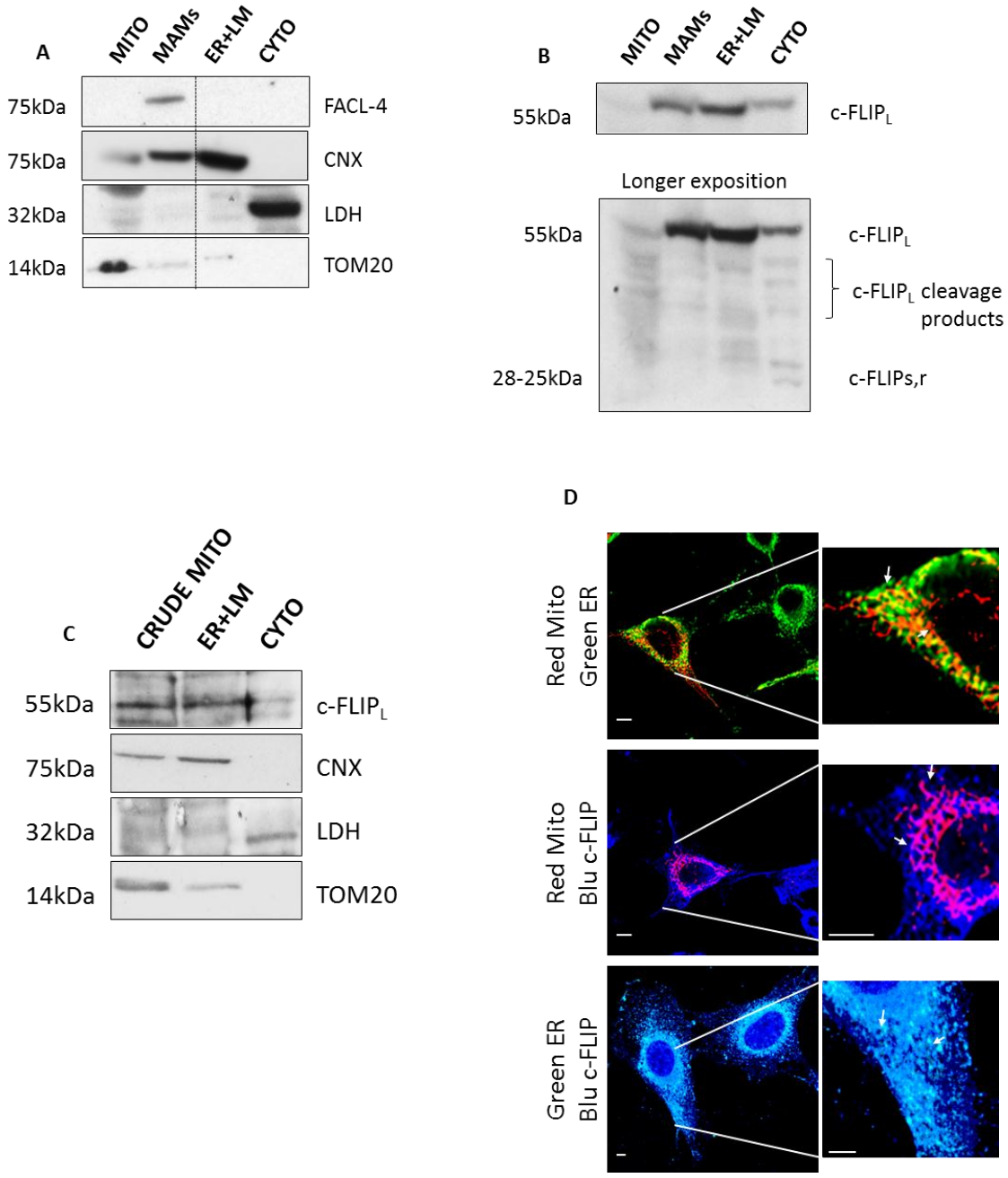

Figure 1. c-FLIP$_L$ localizes at the ER and mitochondria-associated membranes. (A) Proteins (20 µg) from Percoll-purified subcellular fractions of mouse liver, were separated by SDS–PAGE and immunoblotted with the indicated antibodies. **(B)** Localization of endogenous c-FLIP isoforms and cleavage products in subcellular fractions from mouse hepatocytes. **(C)** Western blot of the indicated proteins in subcellular fractions from WT MEFs. **(D)** Representative confocal images of WT MEFs transfected with the indicated plasmids. Cells were fixed and immunostained to detect the endogenous c-FLIP. Boxed areas are magnified 3.

2. c-FLIP depletion results in an altered ER morphology, but intact mitochondria

Ablation of MAMs localized proteins such as MFN2, PACS2 and PERK has shown to alter morphology of both ER and mitochondria, hence influencing the functional and physical coupling of the two organelles. We investigated the role of the ER- and MAM-localized long isoform of c-FLIP in ER and mitochondrial morphology. To this aim we performed three-dimensional (3D) reconstructions of volume rendered confocal stacks of mitochondria- and ER-targeted fluorescent proteins comparing c-FLIP$^{-/-}$ and WT MEFs. As shown in Figure 2A, evaluating length and morphology of mitochondria specifically stained with red fluorescent protein (MTRFP), we did not observe significant differences in mitochondrial morphology and distribution between WT and c-FLIP$^{-/-}$ MEFs. Integrity of the mitochondrial network was also verified by evaluating the total ATP production (Figure 2B), which was similarly produced by both cell lines. Similarly, we did not observe any evident difference in the morphology of Golgi apparatus as shown in Figure 2C. By contrast, we noted an evident alteration in ER morphology of c-FLIP$^{-/-}$ MEFs, when compared to WT counterparts. In WT MEFs, the ER appeared as a network of interconnected tubules and cisternae, spanning the whole cytosolic area. Instead, c-FLIP depleted cells showed a deranged ER, which appeared fragmented and characterized by enlarged cisternae, with an apparent increase in the cisternal versus reticular ER ratio (Figure 2D, upper panels). We also demonstrated the involvement of c-FLIP$_L$ in regulation of ER shape, by re-expressing c-FLIP$_L$ in c-FLIP$^{-/-}$ MEFs. As shown in the lower panels in Figure 2D, whereas transfection of c-FLIP$^{-/-}$ MEFs with a control empty vector (EV) did not induce amelioration of ER structure, re-expression of c-FLIP$_L$ (c-FLIP) partially corrected ER morphology of c-FLIP ablated cells, as supported by both morphological analysis of 3D-reconstructed and volume rendered confocal images. Alterations in ER morphology were further confirmed evaluating the ER luminal contiguity by fluorescence recovery after photobleaching (FRAP) of ER-targeted yellow fluorescent protein (ERYFP). In Figure 2E, we reported that fluorescence recovery of photobleached ERYFP proceeds much more slower in c-FLIP$^{-/-}$ MEFs than in WT cells, suggesting that when c-FLIP is ablated, at cell periphery, the ER organized in large cisternae lacks luminal contiguity. Conversely, when we evaluated the recovery of fluorescence of ERYFP in the perinuclear region, where ER cisternae are usually more distributed, as expected we did not observe significant changes in the luminal contiguity of c-FLIP ablated cells, indicating that ER defects mainly affected its organization at the periphery (Figure 2F). Again, the re-

introduction of c-FLIP$_L$ in ablated MEFs, partially recovered the phenotype observed in c-FLIP$^{-/-}$ cells. Altogether these data indicate a role for c-FLIP$_L$ in regulation of ER dynamics and structure. Our results suggest that c-FLIP$_L$ is critical for ER shaping and integrity, whereas other organelles such as mitochondria and the Golgi are not significantly affected by c-FLIP$_L$ ablation.

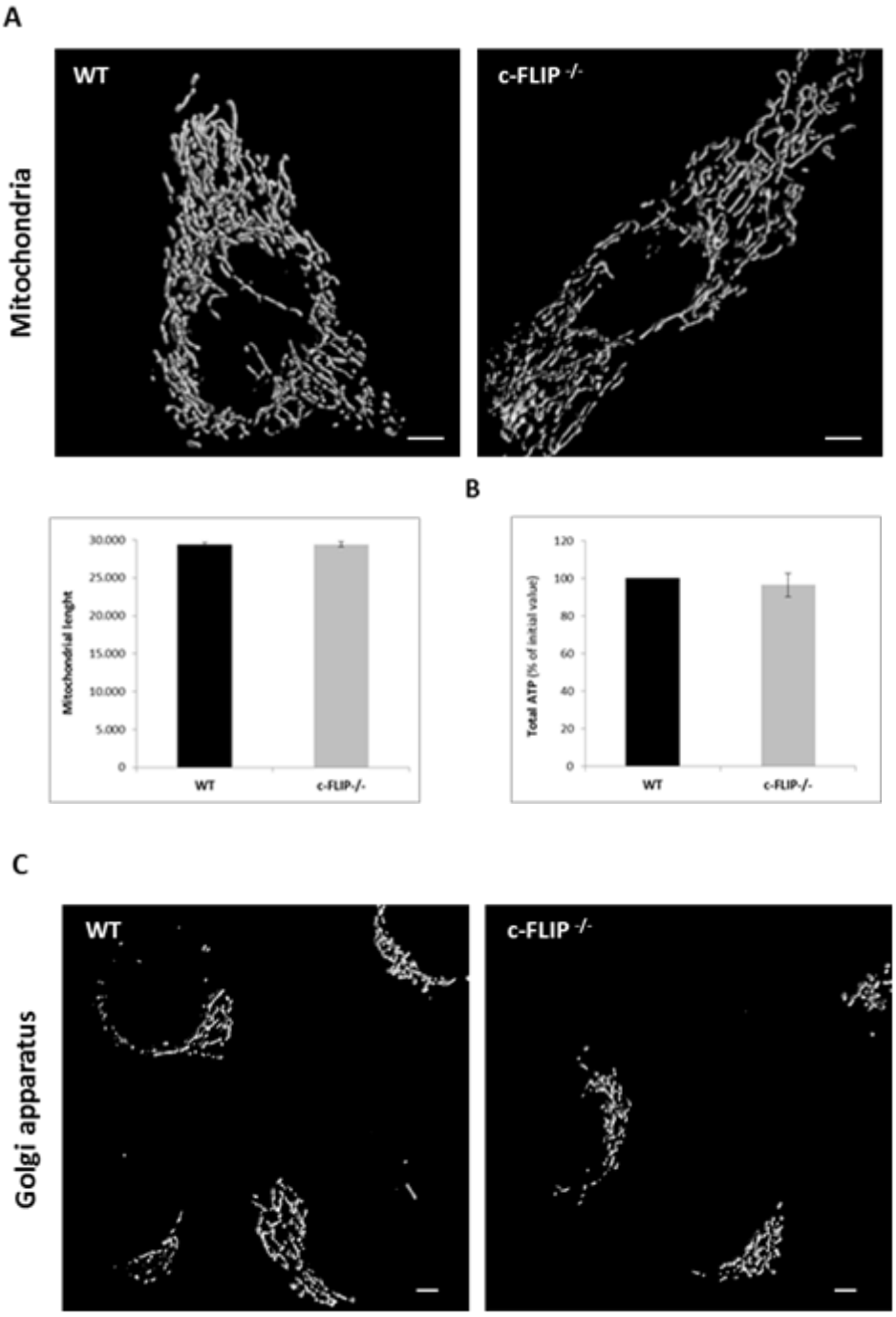

Figure 2. c-FLIP ablation alters ER morphology and luminal contiguity, but not mitochondria and Golgi apparatus. **(A)** Top: representative 3D-reconstructions of mitochondria in MEFs of indicated genotype transfected with MTRFP. Bottom: mean±s.e.m. (n=4, 25 cells per experiment) of data from A. **(B)** Total cellular ATP levels were measured in cells of the indicated genotype. Data represent mean±SEM of 3 independent experiments. MTRFP, mitochondria-targeted ref fluorescent protein. **(C)** Representative 3D-reconstructions of Golgi apparatus in MEFs of indicated genotype stained with the GM130 antibody.

D

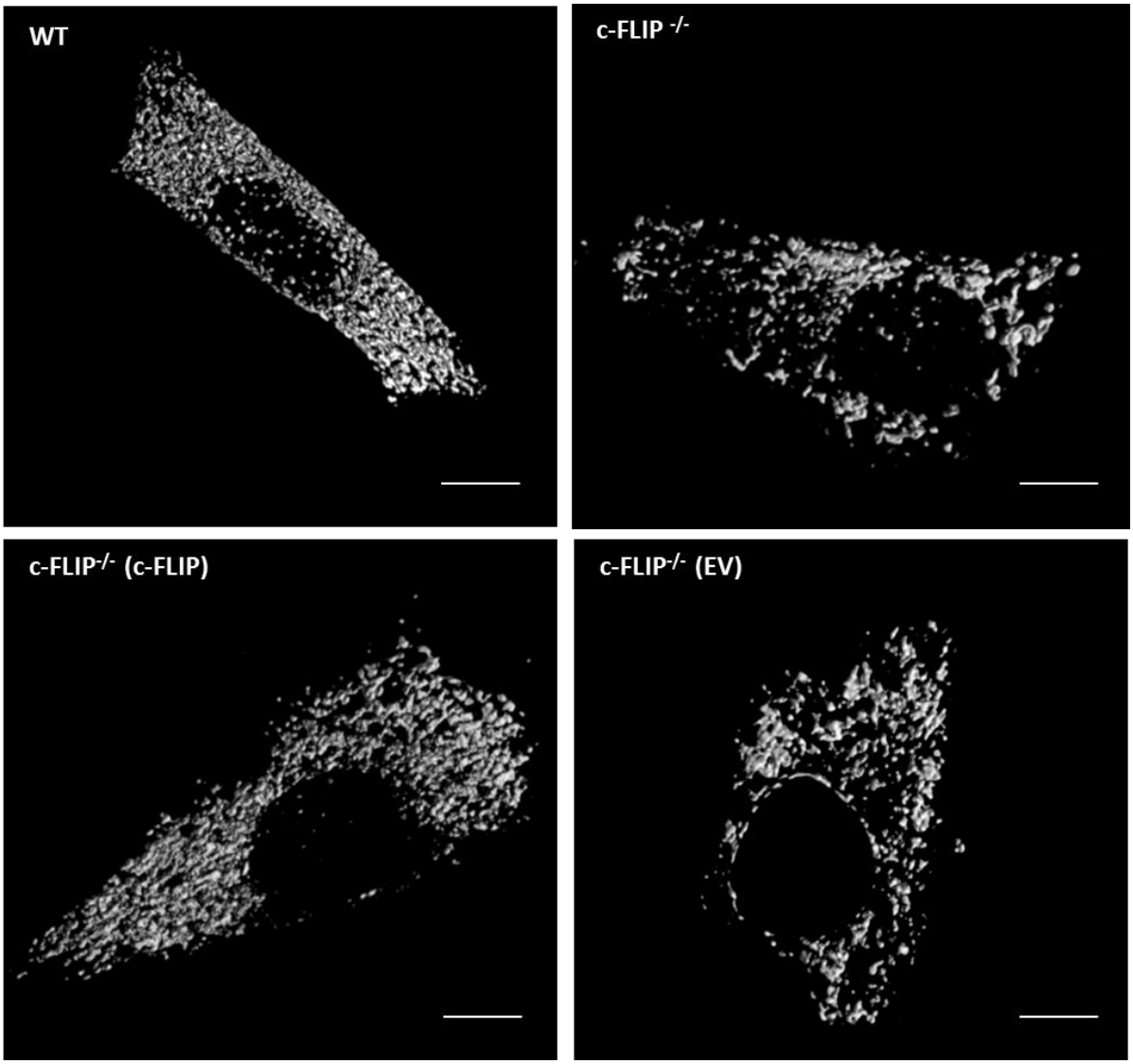

Figure 2. Figure 2. c-FLIP ablation alters ER morphology and luminal contiguity, but not mitochondria and Golgi apparatus. (D) Representative 3D-reconstructions of ER in MEFs of indicated genotype co-transfected with ERYFP and the indicated plasmids. In the upper panels, ER morphology of WT and c-FLIP$^{-/-}$ MEFs was reported. In the lower panel, ER structure of c-FLIP$^{-/-}$ cells transfected respectively with c-FLIP$_L$ and the empty vector (EV) was evaluated.

E

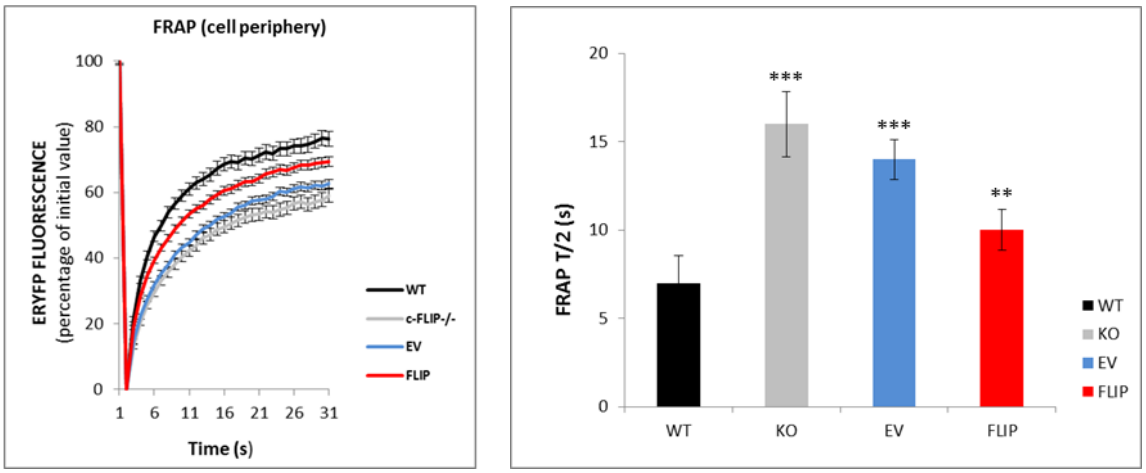

F

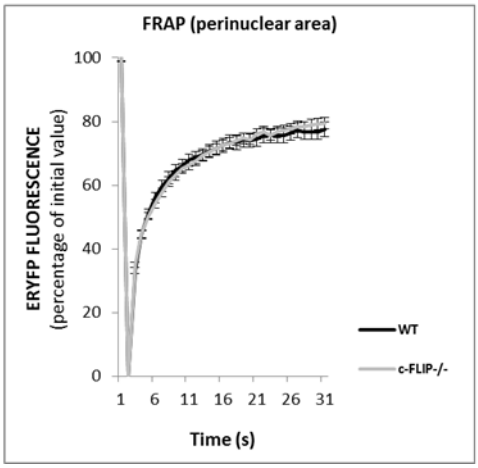

Figure 2. Figure 2. c-FLIP ablation alters ER morphology and luminal contiguity, but not mitochondria and Golgi apparatus. (E) Left: Fluorescence recordings from real-time sequence of ERYFP FRAP in c-FLIP$^{-/-}$ and WT MEFs, in the cell periphery. Right: Mean±s.e.m (n=5, 10 cells per experiment). **(F)** Fluorescence recordings from real-time sequence of ERYFP FRAP in c-FLIP$^{-/-}$ and WT MEFs in the perinuclear regions. 16 μm^2-regions were photobleached for a total of 3 s, using 100% laser power of the 488nm. EV, empty vector. FRAP, fluorescence recovery after photobleaching; ERYFP, ER-targeted yellow fluorescent protein;

3. Alterations in ER-shaping proteins in c-FLIP$^{-/-}$ MEFs

Morphological alterations of c-FLIP$^{-/-}$ MEFs prompted us to evaluate the involvement of ER-shaping proteins that are known to regulate ER dynamics. In fact, in most cells the ER is usually composed of a mixture of interconnected tubules and cisternae and the balance between tubules and sheets largely depends on the relative amount of RTNs/DP1 and sheet-enriched proteins such as CLIMP63. We firstly analyzed the expression levels of ER-localized proteins in total lysates to discriminate whether the apparent increase in cisternal ER in c-FLIP$^{-/-}$ MEFs could be due to an extensive expansion of the entire organelle. As documented in Figure 3A, we did not detect significant differences in the ER markers, Bap31, CNX, CRT and FACL-4. We therefore wondered if the observed defects in ER morphology, could be associated to variations in the expression levels of ER shaping proteins. Consequently, we evaluated by WB the expression of the ER-shaping protein RTN4, the best characterized member of RTNs family, and that of CLIMP63, an ER-sheet resident protein involved in regulation of cisternal ER. We isolated purified fractions from WT and c-FLIP$^{-/-}$ MEFs and probed them for cross-contaminations from mitochondrial and cytosolic components as previously described (Figure 3B). In Figure 3C, we evaluated the expression of RTN4 isoforms A and B and that of the coiled-coil protein CLIMP63 in ER+LMs fractions isolated from both cell lines. As shown, expression of both reticulon-4 isoforms is reduced in c-FLIP$^{-/-}$ with respect to WT cells. By contrast, we did not note variations in expression levels of the coiled-coil protein CLIMP63 between WT and c-FLIP$^{-/-}$ MEFs. Densitometric analysis reported in Figure 3D, confirmed that c-FLIP$^{-/-}$ MEFs presented a lower amount of RTN4 isoforms than WT. Nevertheless, even though an increase in CLIMP63 could not be observed in our model, the unbalance in the RTNs:CLIMP63 ratio could contribute to explain ER defects and the altered equilibrium between reticular ER and ER sheets in c-FLIP$^{-/-}$ MEFs. We also compared the expression of Atlastins (ATLs), another family of ER shaping proteins, which promote the fusion of adjacent ER tubules and whose down-regulation primarily affects Golgi morphology. Accordingly to the intact morphology of Golgi apparatus, WB analysis reported in Figure 3E did not reveal any significant differences in the expression of ATLs isoforms 1 and 2 between WT and c-FLIP$^{-/-}$ MEF. A slight reduction in ATL3 was observed in c-FLIP$^{-/-}$, even though being these three isoforms functionally redundant, we hypothesized that the observed reduction in ATL3 expression was not significant. Taken together, these results hypothesize that alterations in the expression of curvature-inducing proteins such as RTNs could be involved in the regulation of dynamics and tubulation of ER

in c-FLIP$^{-/-}$ MEFs, thus confirming that the enlargement of ER sheets observed in c-FLIP ablated cells could be associated to an unbalanced RTNs:CLIMP63 ratio. Moreover, our findings hypothesize for the first time that a caspases inhibitor is able to affect ER shaping, probably by modulating the cleavage and stability of ER-shaping proteins.

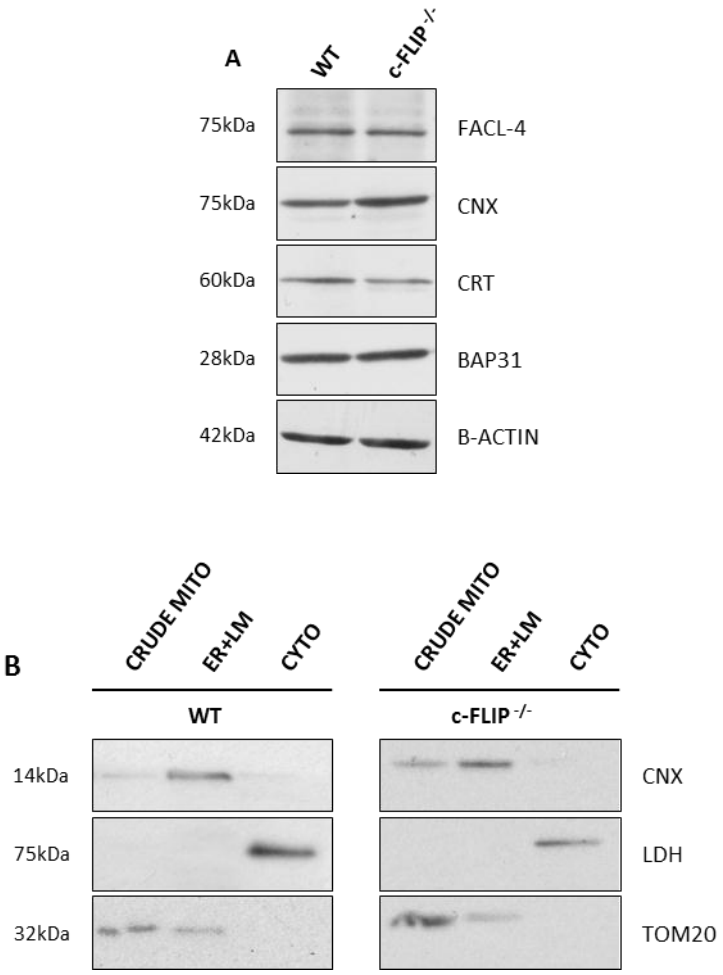

Figure 3. Altered ER morphology in c-FLIP$^{-/-}$ is associated to variations in ER-shaping proteins levels. (A) Total lysates (50µg) from WT and c-FLIP$^{-/-}$ MEFs were separated by SDS-PAGE and blotted for different ER markers. B-actin was used to normalize. **(B)** Proteins (20µg) from crude mitochondria, endoplasmic reticulum (ER+LMs) and cytosol fractions of WT and c-FLIP$^{-/-}$ MEFs were prepared and cross-contaminations were evaluated as reported in Figure 1C.

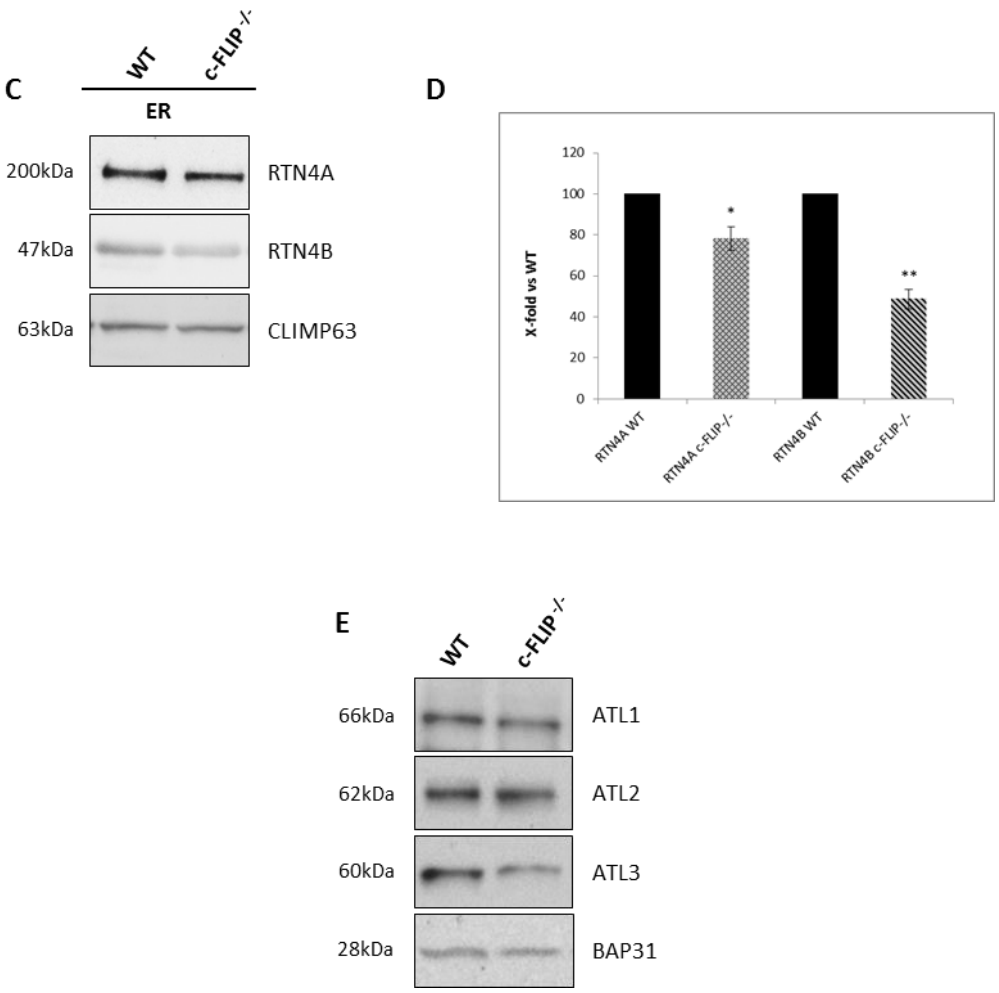

Figure 3. Altered ER morphology in c-FLIP$^{-/-}$ is associated to variations in ER-shaping proteins levels. (C-D) Western Blot and densitometric analysis of expression levels of reticulon4 isoforms (RTN4A,B) and CLIMP63 in ER fractions from WT and c-FLIP$^{-/-}$ MEFs. **(E)** Expression levels of atlastin isoforms 1,2,3 (ATL1,2,3) in ER fractions were evaluated by WB analysis. Bap31 was used as normalizer. (*p≤0,001. **p≤0,0001)

4. Lack of c-FLIP$_L$ alters the ER-mitochondria tethering

As previously described, ablation of c-FLIP in MEFs altered the ER structure, probably due to variations in RTNs levels. The unexpected localization of c-FLIP$_L$ at the ER and MAMs and its role in the regulation of ER morphology, prompted us to address whether c-FLIP$_L$ could also contribute to the ER-mitochondria tethering. Semi-quantitative confocal microscopy analysis of volume-rendered 3D reconstructions of z-axis stacks of confocal images of ERYFP and MTRFP were used to measure the juxtaposition between ER and mitochondria. As shown in Figure 4A, in WT MEFs (top panels, on the left) several yellow areas, that indicate the co-localization of the two organelles, were noticeable. Moreover, the interconnection between mitochondria and the ER network was evident. Conversely, tethering of the two organelles was reduced in c-FLIP$^{-/-}$ MEFs (top panels, on the right), in which ER and mitochondria overlapped to a lower extent. c-FLIP$_L$ re-expression in ablated cells corrected tethering of c-FLIP$^{-/-}$ MEFs, whereas no changes in organelle juxtaposition were observed in c-FLIP$^{-/-}$ transfected with the empty vector (EV). We quantified the ER-mitochondria juxtaposition calculating the Manders' colocalization coefficient [116], a method to measure the degree of co-localization of objects in confocal dual-colour images, and get quantitative information about the positional relation between two biological objects. By this procedure, we revealed a statistical significant, ~20% reduction of the ER-mitochondria tethering in c-FLIP$^{-/-}$ MEFs, that was counterbalanced by c-FLIP$_L$ reintroduction (Figure 4C). We further confirmed the reduced ER-mitochondria tethering, by comparing the contamination of crude mitochondria by light membranes (LMs). To this aim, we used mitochondria isolated from c-FLIP$^{-/-}$ and WT MEFs and probed them for the ER marker CNX. Accordingly with our previous result, as reported in Figure 4A, crude mitochondria from c-FLIP$^{-/-}$ contained a lower amount of CNX, thus suggesting that fractions from depleted cells were less contaminated by LMs than those from WT probably as a consequence of the reduced ability of the two organelles to interact each other. Altogether, our findings suggest that c-FLIP$_L$ positively regulates ER morphology and ER-mitochondria tethering.

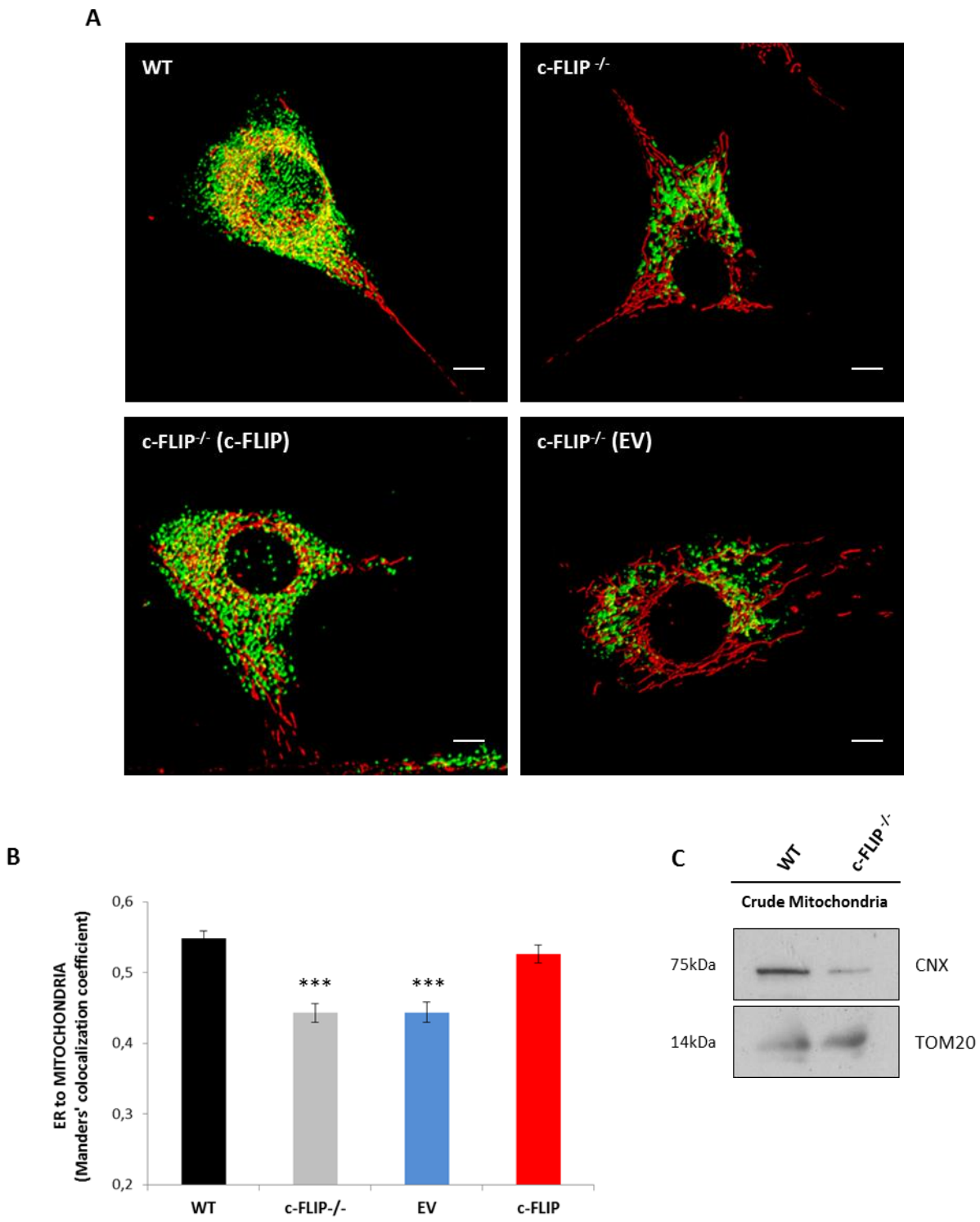

Figure 4. c-FLIP regulates mitochondria–endoplasmic reticulum juxtaposition. (A) 3D-reconstructions of ER and mitochondria in MEFs of indicated genotype co-transfected with MTRFP, ERYFP and the reported plasmids. Yellow areas indicate that organelles are closer than 270 nm. Scale bar, 50 mm. In the lower panels, c-FLIP indicates the re-introduction of c-FLIP$_L$ in depleted MEFs; EV indicates the empty vector. **(B)** Mean±s.e.m. (n=5, 10 cells *per* experiment) of interaction data from B. **(C)** Western blot of the specified proteins in crude mitochondrial fractions isolated from the indicated MEFs. (***p≤0,0001)

5. c-FLIP$^{-/-}$ MEFs are selectively resistant to ER stress mediated apoptosis

ER-mitochondria juxtaposition mediates the apoptotic response to several stimuli, including prolonged ER stress, because a local flux of calcium from the ER towards mitochondria participates to apoptosis induction. Our results suggest that ablation of c-FLIP leads to the disruption of the ER structure, apparently causing dilation of cisternae and fragmentation of ER network. ER membranes expansion occurs even during ER stress [117], and the concomitant increase in the capacity of this organelle has been related to a reduced sensitivity to ER stress inducers [118]. In view of the localization of c-FLIP$_L$ at the ER and MAMs, and its role in modulation of both ER structure and ER-mitochondria tethering, we also investigated its involvement in the ER stress-mediated apoptotic response. To this aim, we treated WT and c-FLIP$^{-/-}$ MEFs with two ER stress inducers thapsigargin (TP), that inhibits the sarcoplasmic/ER Ca^{2+}-ATPase reducing ER Ca^{2+} levels, and tunicamycin (TN), that blocks protein N-glycosylation and export from the ER. After 16h treatment, we measured TP- and TN-mediated cytotoxicity by the colorimetric MTT assay. Surprisingly, we observed that c-FLIP$^{-/-}$ MEFs were less sensitive than WT to prolonged ER stress mediated by both stimuli (Figure 5A). Consequently, we evaluated the apoptotic response assessing cleavage of caspase-3 and PARP with specific antibodies. As shown in Figure 5B, cleavage of both PARP and caspase-3 was more evident in WT cells than in c-FLIP$^{-/-}$ MEFs, confirming the reduced sensitivity of the latter. We therefore wondered whether c-FLIP$^{-/-}$ cells could have adapted to ER stress modulating the expression of ER stress sensors or that of proteins involved in the progression of ER stress response. To this aim, we evaluated the expression of two ER stress markers, the chaperone Bip/Grp78 and the transcription factor CHOP/GADD153, whose overexpression rapidly take place after ER stress induction. In basal conditions, we did not find any noteworthy difference between WT and c-FLIP$^{-/-}$ MEFs neither regarding Bip/Grp78 levels, nor CHOP/GADD153. In accordance, upon treatment with TP and TN, we observed up-regulation of both Bip/Grp78 and CHOP/GADD153 in both WT and c-FLIP$^{-/-}$ MEFs, even though the up-regulation occurred to a different extent in these cells in response to TP and TN (Figure 5B). Successively, to discriminate whether this increased resistance of c-FLIP$^{-/-}$ cells was restricted to ER stress-dependent stimuli, we treated both cell lines with the monoclonal antibody activating Fas (JO-2) to activate the extrinsic pathway of apoptosis, and with etopside to activate the mitochondrial one. As previously described by Yeh, W.C. et al. [25], we confirmed that c-FLIP$^{-/-}$ MEFs were as susceptible as WT cells to stimuli activating the

intrinsic pathway, whereas they displayed higher caspase-3 cleavage as compared to WT, upon triggering of Fas receptor by its agonist (Figure 5C). Together, our results indicate that the reduced sensitivity to ER stress stimuli in c-FLIP ablated cells does not depend on an adaptive down-regulation of ER stress machinery. We can therefore hypothesize that changes in ER morphology or in the ER-mitochondria distance driven by c-FLIP absence, could lead to a less efficient transmission of apoptotic signals to mitochondria, therefore explaining the reduce sensitivity c-FLIP$^{-/-}$ MEFs to TP and TN.

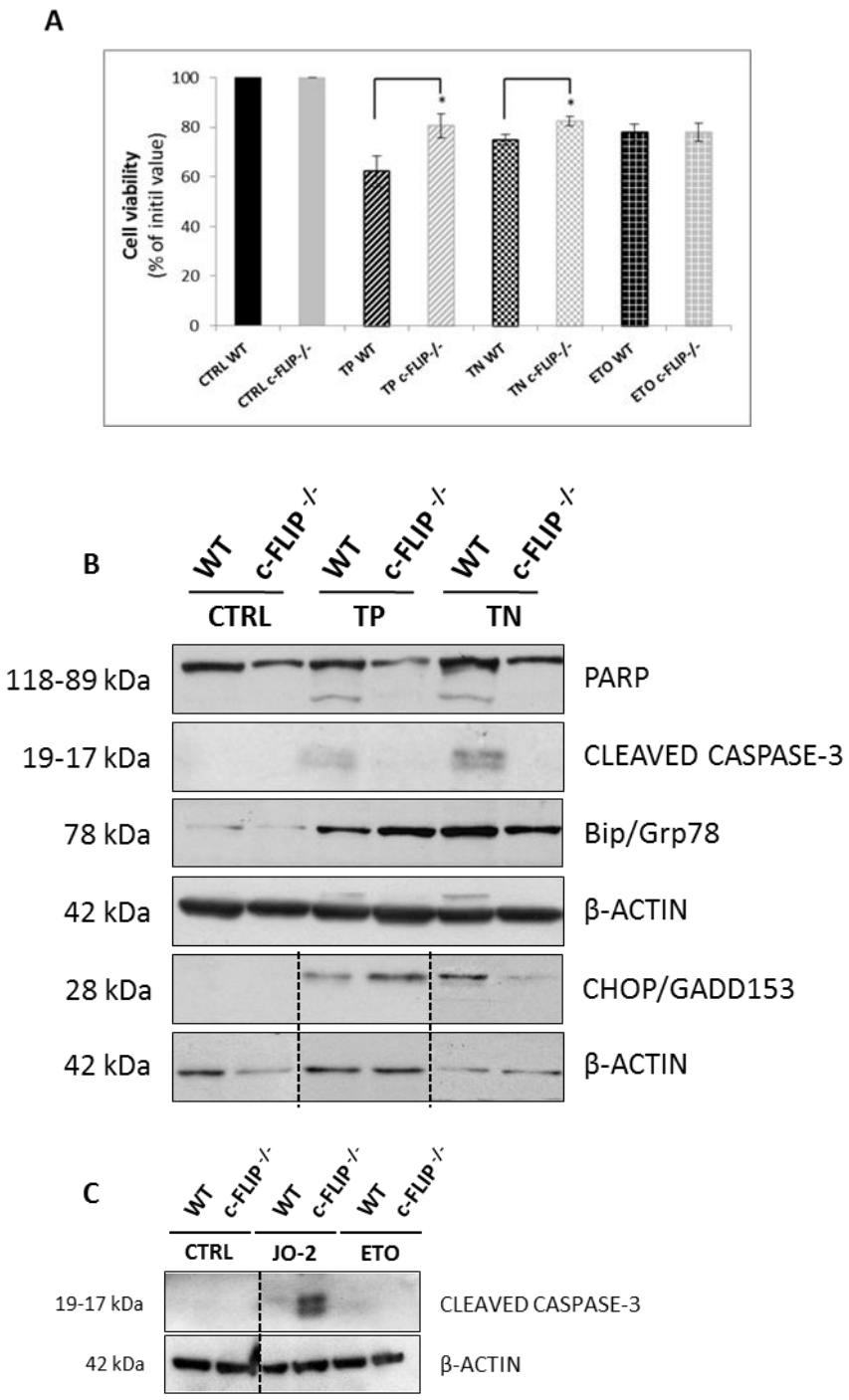

Figure 5. Altered ER stress mediated apoptosis in c-FLIP depleted MEFs. (A) MTT assay establishing citotoxicity of thapsigargin (TP), 0,1mM and tunicamycin (TN), 1µg/µl after 16h of treatment. **(B)** WB analysis of total lysates (40µg) from MEFs of the indicated genotype, upon treatment wit TP and TN. Apoptosis was investigated evaluating cleavage of PARP and caspase-3. ER stress induction was measured evaluating up-regulation of Bip/Grp78 and CHOP/GADD153. **(C)** Evaluation of caspase-3 cleavage by WB analysis in wt and c-FLIP$^{-/-}$ MEFs treated with JO-2 10µg/ml, for 3h and etoposide (ETO) 0,1mM, for 16h. (*p≤0,05)

6. Alterations in calcium signaling in c-FLIP depleted cells

It is known that MAMs ensure Ca^{2+}-exchange between the ER and those mitochondria that reside closely to the ER. In fact, both organelles are enriched in Ca^{2+} signaling elements to permit a fine regulation of calcium fluxes at their interface. Apoptotic stimuli such as prolonged ER stress induce a rapid Ca^{2+} transfer to mitochondria, where calcium ultimately participate to apoptosis induction. We wondered whether the reduced sensitivity of c-FLIP$^{-/-}$ MEFs to ER stress-dependent apoptosis could be related to altered Ca^{2+}-exchange between the two organelles. To investigate the role of c-FLIP in Ca^{2+} homeostasis in our model, we compared Ca^{2+} fluxes in Fura-2-loaded WT and c-FLIP$^{-/-}$ treated with the IP_3-inducing agent ATP and with thapsigargin, a drug that blocks the SERCA pumps on the ER causing the passive discharge of this Ca^{2+} store. EGTA was added to Hanks buffer to perform all experiments in Ca^{2+}-free conditions and assess only intracellular calcium signaling. We firstly stimulated cells with ATP (Fig. 6A), and we observed that the cytosolic Ca^{2+} increase upon stimulation was lower and delayed in c-FLIP$^{-/-}$ as compared to WT cells. Likewise, TP-treated c-FLIP$^{-/-}$ cells displayed a severely blunted Ca^{2+} release from ER, resulting in a lower increase in cytosolic Ca^{2+} with respect to WT counterparts (Figure 6B). TP-dependent passive discharge of ER is an indirect evaluation of the ER Ca^{2+} content. Therefore, altered calcium signals evoked by TP in c-FLIP$^{-/-}$ MEFs suggested that Ca^{2+} concentration in the ER at the steady state was lower in c-FLIP$^{-/-}$ than in WT and it could probably account for the different ATP-induced Ca^{2+} release. In conclusion, taken together these findings hypothesize a role for c-FLIP as regulator of Ca^{2+}-homeostasis at the ER.

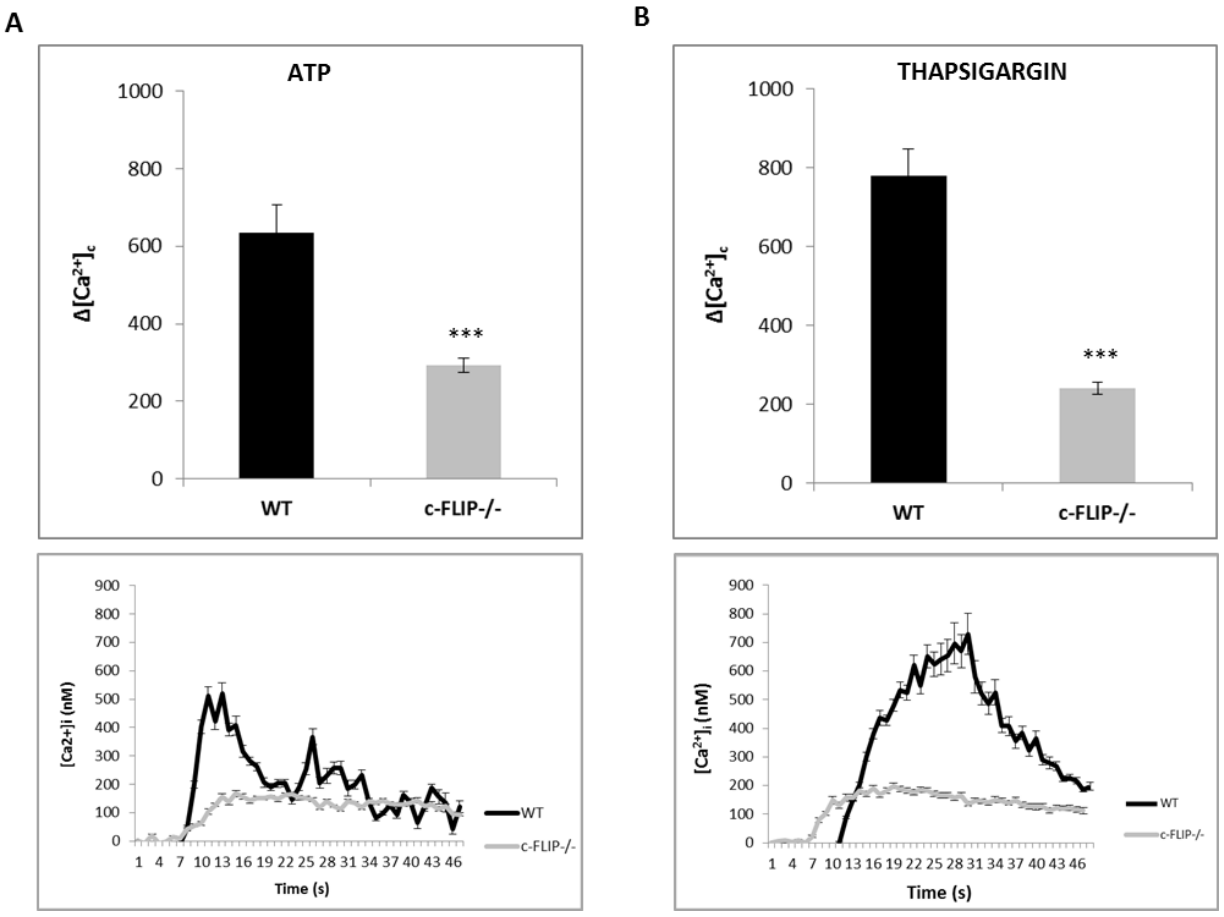

Figure 6. c-FLIP ablated cells present altered Ca^{2+} signaling. (A) Fura-2 recordings of cytosolic Ca^{2+} ($[Ca^{2+}]_c$) after active ER Ca^{2+}-release induced by ATP (0,1mM) in MEFs of the indicated genotype. **Top:** Mean±s.e.m. of n=3 recordings. **(B)** Fura-2 recordings of cytosolic Ca^{2+}($[Ca^{2+}]_c$) after passive discharge of ER Ca^{2+}-stores induced by thapsigargin (0,1mM) in MEFs of the indicated genotype. **Top:** Mean±s.e.m. of n=3 recordings. All the experiments are performed in Ca^{2+}-free solutions. (***$p \leq 0{,}0001$)

7. Increased basal caspase-8 activation in c-FLIP$^{-/-}$ MEFs

It has been previously described that the effector caspase-7 cleaves RTN3 and RTN4B. We therefore wondered if the reduced levels of RTN4 observed in c-FLIP$^{-/-}$ MEFs could be related to an increased caspase-activity and cleavage. We firstly confirmed by the PMAP software the presence of two caspase-cleavage sites in RTN4 sequence (Figure 7A). Successively, we compared the basal caspase-8 activation of WT and c-FLIP$^{-/-}$ cells. As shown in Figure 7B, we observed an enhanced caspase-8 activation in c-FLIP$^{-/-}$ as compared to WT MEFs under basal conditions. Treatment of both WT and c-FLIP depleted cells with a specific-caspase-8 inhibitor for 48h induced a reduction of basal caspase-8 activity to levels comparable to WT (Figure 7B). We therefore hypothesized that c-FLIP re-introduction in depleted cells could similarly reduce activation of caspase-8. In agreement, preliminary results suggested that after c-FLIP expression, caspase-8 activity was reduced to levels similar to those induced by the specific inhibitor. Taken together these results confirm that ablation of c-FLIP in MEFs enhances the basal activation of caspase-8, even though such up-regulation is not consistent with apoptosis onset, as deducible by the evaluation of caspase-3 cleavage in control conditions reported in Figure 5B. However, increased caspase-8 activity in c-FLIP$^{-/-}$ MEFs could be sufficient to increase caspase-7 activation, therefore inducing the cleavage, and therefore the reduction, of RTN4 in these cells.

A

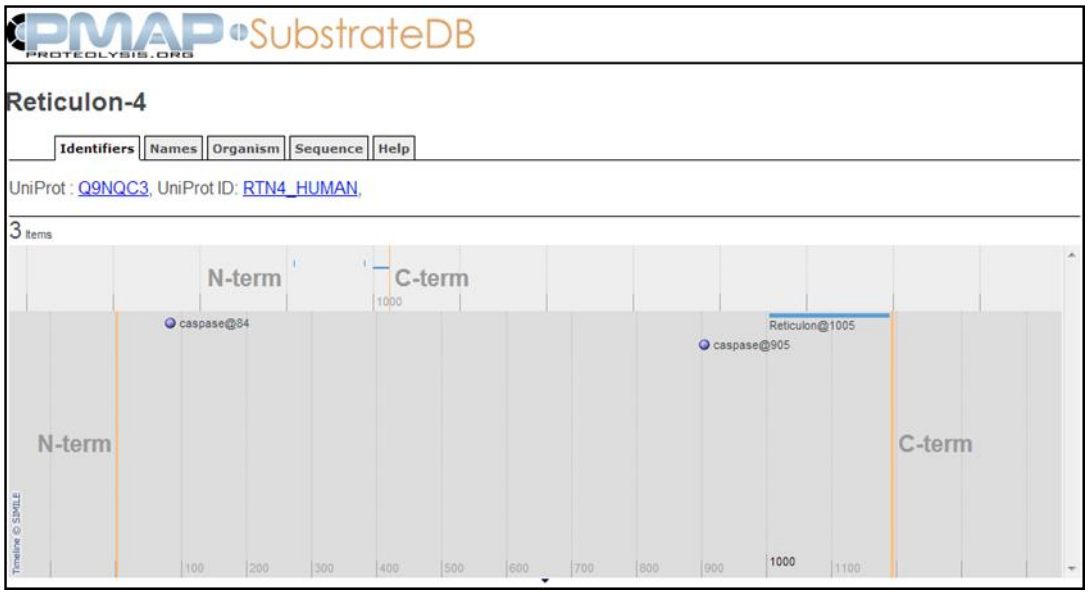

B

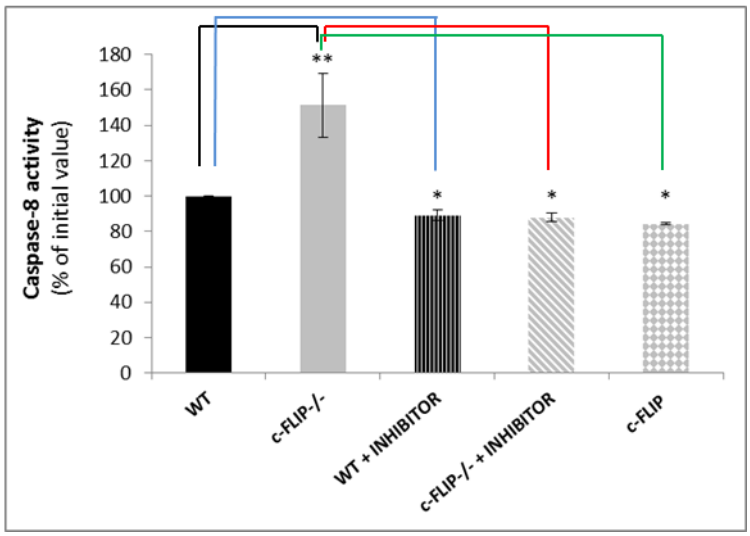

Figure 7. Caspase-8 activity is increased in c-FLIP$^{-/-}$ cells. (A) Analysis of caspase-cleavage sites on reticulon-4 sequence using The Proteolysis MAP (PMAP). **(B)** Caspase-8 activity was measured in c-FLIP$^{-/-}$ and WT MEFs in basal conditions and after treatment with a specific caspase-8 inhibitor (10µM) for 48h. (*p≤0,05. **p≤0,01)

DISCUSSION

During apoptosis, the DISC complex is assembled within LRs on the plasma membrane. More recently, several groups independently identified components of the death receptor-signaling on membranes of both mitochondria and ER, where caspase-8 and FADD interact with resident proteins or lipids, forming local complexes. On both these organelles, intracellular LR-like microdomains have been detected, therefore suggesting that molecular platforms could be formed in these regions in order to locally activate caspase-8 and cleave different targets directly where needed. LR-like microdomains localize at the so-called MAMs, at the ER-mitochondria interface, and similarly to lipid-rafts in the plasma membrane, their liquid-ordered structure is necessary to recruit and orientate signaling complexes involved in regulation of cell metabolism, Ca^{2+}-homeostasis and apoptosis [54]. In this study we investigated the localization of the inhibitor of caspase-8, named c-FLIP, finding out that, similarly to caspase-8 and FADD, c-FLIP is not only cytosolic and nuclear as previously described, but it also resides in membranous organelles. Indeed, here we demonstrate the presence of the long isoform of c-FLIP in the ER and MAMs, but not in isolated mitochondria. To our knowledge, it is the first time that c-$FLIP_L$ is clearly identified at the level of a membranous organelle, even though the existence of a pool of c-FLIP associated to intracellular membranes was previously reported by Shain, K.H. et al. [119]. These authors, showed that c-$FLIP_L$ was predominantly membrane-bound under basal conditions, while it increased in the cytosol and in the plasma membrane-associated DISC upon apoptotic stimulation, suggesting that the modulation of its distribution could be a crucial mechanism for regulating cellular responses to an apoptotic stimuli. Recruitment of c-FLIP to the cytosol or plasma membrane upon stimulation could also explain the delay in its identification in the ER. In fact, most of the studies regarding c-FLIP have aimed at studying cancer cell death after pro-apoptotic treatments, which could in turn cause the re-distribution of c-FLIP from membranous organelles to a cytosolic localization.

ER and mitochondria are largely involved in the regulation of cell death and the importance of functional crosstalk between these two organelles is now evident. As previously described in the introduction section, several apoptosis regulators localize or are recruited at the ER-mitochondria interface. Moreover, organelle remodeling and modulation of Ca^{2+}-signaling influence the exchange of signals between ER and mitochondria and thus the sensitivity to

different stimuli. Ablation of proteins resident in the MAMs and/or on the ER/mitochondrial side has been often associated to alterations in organelles morphology. In agreement with these observation, we demonstrated for the first time that c-FLIP ablation in mouse embryonic fibroblasts, derived from the lethal knockout mouse model, caused a dramatic remodeling of ER morphology, inducing the enlargement of ER cisternae to the detriment of peripheral, reticular ER. Re-introduction of the ER- and MAM-localized c-FLIP$_L$ in ablated cells partially restored ER morphology, suggesting that the observed phenotype was consequent to the depletion of this protein, and not merely correlated to an adaptive response occurred in the knockout model.

In order to investigate the possible molecular mechanism responsible for ER alterations, we evaluated at biochemical level the expression of proteins involved in ER remodeling. In particular, in c-FLIP$^{-/-}$ cells we observed the reduction of the ER-shaping protein RTN4, whereas we did not notice any variation in CLIMP63, the main component of ER cisternae. A reduction in ER-shaping proteins such as RTNs, or an unbalance in the ratio between these and the coiled-coil proteins such as CLIMP63 have been described to cause alterations of ER structure similar to the phenotype observed in c-FLIP$^{-/-}$ MEFs, therefore confirming our findings.

Ablation of proteins and complexes localized at MAMs was also previously reported to alter ER-mitochondria tethering, besides organelles morphology. Moreover, it was recently demonstrated that yeast strains lacking both components of the tethering complex ERMES and tubule-inducing proteins Rtn1p/Yop1 and Rtn1p/Sey1p display reduced ER-mitochondria contacts and functional communications [120]. These defects were restored by artificial tethering of the two organelles, therefore suggesting that the maintenance of a correct ER structure could contribute to both physical tethering and functional coupling of ER and mitochondria. In agreement with these former studies, after having demonstrated the endogenous localization c-FLIP at MAMs, we observed a reduction in ER-mitochondria tethering in c-FLIP$^{-/-}$ cells, which is partially recovered by re-introduction of c-FLIP$_L$. However, although we can affirm that restoring c-FLIP$_L$ expression in c-FLIP$^{-/-}$ MEFs, ER-mitochondria vicinity increases, we can only speculate that such increased tethering is consequent to the observed recovery in ER structure. Further studies are in fact necessary to clarify the connection between ER morphology and tethering to mitochondria.

It has also been reported that alterations in the ER-mitochondria distance influence functional communications between the two organelles. In fact, the depletion of MAM-localized proteins such as PACS2 and PERK, uncouples these organelles, therefore reducing the transmission of

pro-apoptotic signals to mitochondria and apoptosis onset [103, 121]. In agreement, c-FLIP$^{-/-}$ cells showed ER-mitochondria uncoupling which correlates with a reduced sensitivity to stimuli inducing prolonged ER stress as compared to WT cells. However, differently from PACS2 depleted cells, in which the uncoupling of ER and mitochondria compromises ER homeostasis, c-FLIP depletion does not induce ER stress. Indeed, basal levels of the ER stress sensor Bip/Grp78 did not display differences between c-FLIP$^{-/-}$ and WT cells, indicating that the reduced sensitivity of depleted cells was not ascribable to a basal up-regulation of ER stress machinery. In addition, both WT and c-FLIP$^{-/-}$ showed a rapid increase in the expression of both Bip/Grp78 and CHOP/GADD153 upon ER stress induction, confirming the integrity of ER stress-pathways and thus suggesting that a block in the transmission of the pro-apoptotic signal to mitochondria, which ultimately execute cell death, has occurred in c-FLIP$^{-/-}$ MEFs. In response to tunicamycin treatment, up-regulation of both Bip and CHOP in c-FLIP$^{-/-}$ cells occurred, even though to lower degree with respect to thapsigargin treatment in the same cells. Although both drugs induce ER stress, this discrepancy could be related to the mechanism of ER stress induction mediated by different drugs. In particular, tunicamycin causes proteins accumulation in the ER by blocking their N-glycosylation and transfer to Golgi apparatus. Membrane expansion occurs during ER stress and have been related to the increased tolerance to saturation of ER folding capacity [118]. We can therefore hypothesize that the basal expansion of rough, cisternal ER in c-FLIP$^{-/-}$ cells could render these cells more tolerant to tunicamycin than to thapsigargin treatment, therefore promoting a less efficient or a slower up-regulation of ER stress machinery.

We also observed that Ca^{2+}-release evoked by ATP was reduced in c-FLIP$^{-/-}$ MEFs. Mitochondrial calcium overload is a potent apoptosis inducer and conditions that reduce the transfer of calcium to mitochondria block apoptosis execution. Ca^{2+}-handling complexes at MAMs influence Ca^{2+}-transfer to mitochondria, that is mainly promoted by IP_3-receptors. The reduced ER Ca^{2+}-release observed in c-FLIP$^{-/-}$ could therefore contribute to the increased resistance of these cells to prolonged ER stress, because of the lower Ca^{2+}-transfer to mitochondria. In accordance with this hypothesis, WT and c-FLIP$^{-/-}$ MEFs treated with the cytotoxic, anti-cancer drug, etoposide did not display significant differences in the apoptotic response, suggesting that the intrinsic apoptotic machinery is intact. We also observed that c-FLIP$^{-/-}$ cells showed reduced passive ER discharge with respect to WT. This finding suggested that c-FLIP$^{-/-}$ cells could have a lower amount of calcium in the ER at the steady state, which can in turn account for the reduced IP_3-dependent Ca^{2+}-release. Such hypothesized depletion of ER Ca^{2+}-stores in c-FLIP$^{-/-}$ is however contrasting with previous

findings reporting that the ER depletion is usually associated to the up-regulation of components of the ER stress machinery. Further studies are ongoing to deepen our knowledge regarding alterations in Ca^{2+} levels and signaling in c-FLIP$^{-/-}$ MEFs.

It was previously demonstrated that caspase-7, an effector caspase activated by the apical caspase-8, cleaves RTN3 and RTN4B [122]. Moreover, it was also reported that effector caspase-3 and -7 exert their functions in different subcellular compartments, being active caspase-3 mostly cytosolic and active caspase-7 almost exclusively associated to mitochondrial and microsomal fractions [123]. Furthermore, FADD, which acts in the recruitment of procaspase-8 to the DISC, has been reported to interact with RTN3, forming an ER-bound signaling complex [47]. We wondered if the reduced amount of RTN4 isoforms observed in c-FLIP depleted cells could be related to increased caspase-dependent cleavage of this protein. We confirmed the presence of caspase-cleavage sites in RTN4 sequence by PMAP software. Accordingly to PMAP, the two identified sites are located at N- and C-terminal of RTN4, which are both exposed to cytosol and are therefore accessible to caspases. We also compared basal caspase-8 activation in c-FLIP$^{-/-}$ and WT MEFs, finding out that knockout MEFs showed a higher basal activity of caspase-8, as expected in cells lacking the principal inhibitor of this caspase. We therefore hypothesize that the increased caspase-8 activity in c-FLIP$^{-/-}$ cells could indirectly contribute to reduce RTN4 levels by increasing its cleavage, probably forming complexes at the ER-mitochondria interface. In agreement, both RTN4 itself and CLIMP63 have been reported at the MAMs [55]. We also preliminary observed that re-introduction of c-FLIP reduces basal caspase-8 activation to levels comparable to those of WT and c-FLIP$^{-/-}$ treated with a specific caspase-8 inhibitor. In accordance with our hypothesis, re-expression of c-FLIP leads to the restoration of ER morphology and tethering. Additional experiments are ongoing to evaluate the correlation between c-FLIP$_L$ levels and RTN4 cleavage. Although further studies are necessary to clarify the role of caspases in the regulation of organelles morphology, these data together support an unexpected role for c-FLIP at the ER-mitochondria interface. We believe that c-FLIP represents a novel component of molecular platforms localized at MAMs. The presence of c-FLIP, as well as that of other DISC components, at ER and mitochondria highlights for DISC proteins unexpected roles different from their canonical function as extrinsic apoptosis regulators. Since caspase-8 inhibition in the whole cells is not desirable because it would have deleterious implications for cell proliferation, we believe that finely controlled caspase-8 activation could be important for the processing of specific targets where needed. In this view, c-FLIP would act as inhibitor of caspase-8 at the MAMs, by regulating the caspase-mediated

processing of local substrates. By this local and specific mechanism c-FLIP could therefore control ER morphology, ultimately contributing to physical and functional coupling of this organelle to mitochondria.

MATERIALS AND METHODS

Cell culture and transfection

Wild type (WT) and c-FLIP$^{-/-}$ mouse embryonic fibroblasts (MEFs) were a generous gifts of Wen-Chen Yeh, Amgen Institute, Toronto, Canada. The MEFs were cultured in DMEM, enriched with 10% fetal bovine serum, glutamine (2 mmol/L), sodium pyruvate (1 mmol/L), and non-essential amino acids, in the presence of penicillin (100 U/ml) and streptomycin (100 µg/ml). Transfections whit pDsRed2-Mito (Clontech), pEGFP-ER (Clontech) and pBluescript or c-FLIP$_L$ plasmid were performed using Transfectin reagent (BIORAD) at 2µg/µl, accordingly to the manufacturer's instructions.

Subcellular Fractionation

Whole mouse liver or WT and cFLIP$^{-/-}$ MEFs obtained from 4, confluent, 500cm^2 petri dishes were washed twice with PBS, re-suspended in isolation buffer (IB, 200 mM sucrose, 1mM EGTA-Tris, and 10 mM Tris-MOPS, pH 7.4), and then broke up by dounce homogenization. Accordingly to Frezza C., et al. [124], the homogenized suspension was spun at 800g for 10 min at 4°C, to pellet nuclei and cell debris; the supernatant was recovered and further centrifuged for 10 min at 10000g, at 4°C. The crude mitochondrial fraction was collected from the pellet, whereas the supernatant was further centrifuged for 30 min at 100,000g. The resulting pellet, mainly enriched in endoplasmic reticulum (ER), but containing other cellular membranes, collectively named light membranes (LM), and the supernatant (cytosolic fraction) were spun again at 100,000g for 30 min at 4°C to increase pureness of the two fractions. The crude mitochondrial fraction was further purified by resuspending it in a 2X volume of IB and then centrifuged three times at 10000g for 10 minutes, at 4°C. Mitochondria were finally purified from MAMs contamination by centrifugation at 95000g for 30 minutes at 4°C, on a 30% Percoll gradient in IB. The obtained pure mitochondria, recovered as the lowest layer on the Percoll gradient, were washed and resuspended in IB. Conversely, MAMs were identified as the layer overlying the mitochondrial fraction on the Percoll gradient.

Protein concentration was determined by BCA assay (Pierce) and 20 μg of protein were separated by SDS-PAGE and immunoblotted for the indicated antibodies as indicated.

Analysis of cell viability

10^4 WT and c-FLIP$^{-/-}$ MEFs were seeded on 96-wells plate. 24h after the seeding, cells were treated with the ER stress inducers thapsigargin (Sigma-Aldrich), 1μM and tuncamycin (Sigma-Aldrich), 1μg/μl for 16h. Cell viability was assessed by 3-(4,5-dymethyl thiazol 2-y1)-2,5-diphenyl tetrazolium bromide (MTT, Sigma-Aldrich), according to [125]. After MTT addition in DMEM medium, without FCS, cells were incubated for 4h at 37°C; medium was then removed and 100μl of 2-propanol (Sigma-Aldrich) were added to each well to solubilize the blue crystals. The OD at 550 nm were then determined for the contents of each well.

ATP measurement

Total ATP levels were measured by using the ATP detection assay system ATPlite (PerkinElmer), according to manufacturer's protocol. ATP levels were normalized by total protein concentration.

Immunoblotting

At the time reported in figures legend, cells were harvested and disrupted in lysis buffer (Cell Signaling) in the presence of complete protease-inhibitor mixture (Sigma). Protein concentration was determined by BCA assay and the indicated proteins were separated by SDS-PAGE, transferred onto polyvinylidene difluoride (PVDF, BioRad) or nitrocellulose membranes (Amersham). Membranes were probed using the following antibodies: anti-β-actin (1:10000, SIGMA); anti-calnexin (1:2000, Abcam); anti-Tom20 (1:10000, Santa Cruz Biotechnology); anti-LDH (lactate dehydrogenase, 1:2000, Rockland); anti-FACL4 (1:500, Santa Cruz Biotechnology); anti-calreticulin (1:1000; Abcam); anti-cFLIP, Dave-2, (1:800, Alexis); anti-RTN4A/B (1:1000, Abcam); anti-CLIMP63 (1:1000, Proteintech); anti-

Bip/GRP78 (1:1000, BD Bioscience); anti-CHOP (1:1000, Cell Signaling); anti-cleaved caspase-3 (1:500, Cell Signaling), anti-PARP (1:1000; Cell Signaling).

Immunofluorescence

$5x10^4$ MEFs of the indicated genotype grown on 24-mm round coverslips, were transfected as indicated and fixed after 48h. To visualize c-FLIP and calreticulin distribution, cells were fixed for 30 min at RT with 4% ice-cold paraformaldehyde in PBS (pH 7.4), permeabilized for 10 min with PBS, 0,2% Triton-100 and blocked for 1 h with the blocking solution PBS, 10% BSA. Subsequently cell were incubated overnight at 4°C with antibodies for c-FLIP (1:100, Abcam) or calreticulin (1:100, Abcam), in PBS, 10% BSA. Primary antibodies were revealed incubating for 20 min at RT with an anti-rabbit or anti-mouse IgG conjugated to the fluorochrome indicated in the figure legend. For the detection, a Leica confocal microscope (Laser Scanning TCS SP2) equipped with Ar/ArKr and He/Ne lasers and with a 40X oil 1.40 plan apo immersion objective was utilized.

Imaging

For confocal imaging and analysis of the morphology and tethering of ER and mitochondria, cells seeded onto 24-mm round glass coverslips and incubated in Hanks balanced salt solution (HBSS), supplemented with 10 mM Hepes, were placed on the stage of a Nikon Eclipse TE300 inverted microscope equipped with a spinning-disk PerkinElmer Ultraview LCI confocal system, a piezoelectric z-axis motorized stage (Pifoc, Physik Instrumente, Germany), and an Orca ER 12-bit charge-coupled device camera (Hamamatsu Photonics, Japan). Cells expressing ERYFP and/or MTRFP were excited using the 488 nm or the 543 nm line of the HeNe laser (PerkinElmer) by using a 60x 1.4 NA Plan Apo objective (Nikon). For confocal z-axis stacks, images separated by 0.2 μm along the z-axis were acquired. 3D-reconstruction and volume rendering of the stacks were performed with the appropriate plugins of ImageJ software.

Morphometric and Contact Analysis

Analysis of the interactions between ER and mitochondria in WT and c-FLIP$^{-/-}$ MEFs expressing MTRFP and ERYFP were performed with ImageJ. Deconvolution, 3D-reconstruction and surface rendering were realized using the VolumeJ plugin of ImageJ. Analysis of the interaction between ER and mitochondria was performed using Manders' colocalization coefficient [116].

Fluorescence Recovery After Photobleaching (FRAP)

Cells were plated and transfected with ERYFP as previously described. After 48 h they were incubated in HBSS and placed on the stage of a laser scanning microscope (TCS SP5, Leica). Using the LasAF software (Leica), 16 μm^2-regions were manually defined to be bleached. To bleach the YFP fluorescence, 1 z-plane was bleached for a total of 3 s using 100% laser power of the 514 nm laser line with a 63X, 1.4NA objective. The post-bleaching images were taken at 0,937 s intervals for a total of 120 s. Intensities of the photobleached regions were measured and normalized to the intensities of the same region before photobleaching.

Ratiometric measurement of cytosolic Ca^{2+} concentration

15x10^4 WT and c-FLIP$^{-/-}$ MEFs were seeded on 35mm Petri dishes. 24h after the seeding, cells were incubated at 37°C in culture medium containing 3,5 μM Fura2-AM (Invitrogen). After 45 min, cells were washed free of Fura2-AM and Hanks balanced solution (HBSS, 130mM NaCl, 5,2mM KCl, 1mM $MgCl_2$, 10mM glucose, 10mM HEPES, pH 7.4) was added. EGTA was added to all solutions. Dishes were placed into a culture chamber at 37°C on the stage of an inverted fluorescence microscope (Nikon TE2000E), and connected to a cooled CCD camera (512B Cascade; Roper Scientific). Samples were illuminated alternately at 340 and 380 nm using a random access monochromator (Photon Technology International) and emission was detected using a 510 nm emission filter. Images were acquired (1-ratio image/s) using Metafluor software (Universal Imaging Corporation). Calibration was obtained at the end of each experiment by maximally increasing intracellular Ca^{2+}-dependent fura-2-AM fluorescence with 5μM ionomycin, followed by recording minimal fluorescence in a Ca^{2+}-free medium. $[Ca^{2+}]_I$ was calculated according to the formulas previously described [126].

Evaluation of caspase-8 activity

Caspase-8 activity was measured by the colorimetric FLICE/Caspase-8 Assay kit (BioVision). WT and c-FLIP$^{-/-}$ MEFs were plated on 35-mm Petri dishes. 24h after seeding, where indicated, 10μM caspase-8 inhibitor (InSolution Caspase-8 inhibitor II, Calbiochem) was added in culture medium. 48h later caspase-8 activity was measure according to manufacturer's protocol. Levels of caspase-8 activation were normalized by total protein concentration.

BIBLIOGRAPHY

1. **Kerr, J.F., A.H. Wyllie, and A.R. Currie, *Apoptosis: a basic biological phenomenon with wide-ranging implications in tissue kinetics.* Br J Cancer, 1972. 26(4): p. 239-57.**
2. **Ziegler, U. and P. Groscurth, *Morphological features of cell death.* News Physiol Sci, 2004. 19: p. 124-8.**
3. **Riedl, S.J. and Y. Shi, *Molecular mechanisms of caspase regulation during apoptosis.* Nat Rev Mol Cell Biol, 2004. 5(11): p. 897-907.**
4. **Bouillet, P. and L.A. O'Reilly, *CD95, BIM and T cell homeostasis.* Nat Rev Immunol, 2009. 9(7): p. 514-9.**
5. **Salvesen, G.S. and V.M. Dixit, *Caspase activation: the induced-proximity model.* Proc Natl Acad Sci U S A, 1999. 96(20): p. 10964-7.**
6. **Ow, Y.P., et al., *Cytochrome c: functions beyond respiration.* Nat Rev Mol Cell Biol, 2008. 9(7): p. 532-42.**
7. **Ozoren, N. and W.S. El-Deiry, *Cell surface Death Receptor signaling in normal and cancer cells.* Semin Cancer Biol, 2003. 13(2): p. 135-47.**
8. **Guicciardi, M.E. and G.J. Gores, *Life and death by death receptors.* FASEB J, 2009. 23(6): p. 1625-37.**
9. **Chaigne-Delalande, B., J.F. Moreau, and P. Legembre, *Rewinding the DISC.* Arch Immunol Ther Exp (Warsz), 2008. 56(1): p. 9-14.**
10. **Ozturk, S., K. Schleich, and I.N. Lavrik, *Cellular FLICE-like inhibitory proteins (c-FLIPs): fine-tuners of life and death decisions.* Exp Cell Res, 2012. 318(11): p. 1324-31.**
11. **Thome, M., et al., *Viral FLICE-inhibitory proteins (FLIPs) prevent apoptosis induced by death receptors.* Nature, 1997. 386(6624): p. 517-21.**
12. **Irmler, M., et al., *Inhibition of death receptor signals by cellular FLIP.* Nature, 1997. 388(6638): p. 190-5.**
13. **Hu, S., et al., *I-FLICE, a novel inhibitor of tumor necrosis factor receptor-1- and CD-95-induced apoptosis.* J Biol Chem, 1997. 272(28): p. 17255-7.**
14. **Golks, A., et al., *c-FLIPR, a new regulator of death receptor-induced apoptosis.* J Biol Chem, 2005. 280(15): p. 14507-13.**
15. **Kataoka, T. and J. Tschopp, *N-terminal fragment of c-FLIP(L) processed by caspase 8 specifically interacts with TRAF2 and induces activation of the NF-kappaB signaling pathway.* Mol Cell Biol, 2004. 24(7): p. 2627-36.**
16. **Golks, A., et al., *The c-FLIP-NH2 terminus (p22-FLIP) induces NF-kappaB activation.* J Exp Med, 2006. 203(5): p. 1295-305.**

17. **Katayama, R., et al.,** ***Modulation of Wnt signaling by the nuclear localization of cellular FLIP-L.*** **J Cell Sci, 2010. 123(Pt 1): p. 23-8.**
18. **Zhang, J., et al.,** ***Nuclear localization of c-FLIP-L and its regulation of AP-1 activity.*** **Int J Biochem Cell Biol, 2009. 41(8-9): p. 1678-84.**
19. **Scaffidi, C., et al.,** ***The role of c-FLIP in modulation of CD95-induced apoptosis.*** **J Biol Chem, 1999. 274(3): p. 1541-8.**
20. **Chang, D.W., et al.,** ***c-FLIP(L) is a dual function regulator for caspase-8 activation and CD95-mediated apoptosis.*** **EMBO J, 2002. 21(14): p. 3704-14.**
21. **Micheau, O., et al.,** ***The long form of FLIP is an activator of caspase-8 at the Fas death-inducing signaling complex.*** **J Biol Chem, 2002. 277(47): p. 45162-71.**
22. **Boatright, K.M., et al.,** ***Activation of caspases-8 and -10 by FLIP(L).*** **Biochem J, 2004. 382(Pt 2): p. 651-7.**
23. **Peter, M.E.,** ***The flip side of FLIP.*** **Biochem J, 2004. 382(Pt 2): p. e1-3.**
24. **Yu, J.W. and Y. Shi,** ***FLIP and the death effector domain family.*** **Oncogene, 2008. 27(48): p. 6216-27.**
25. **Yeh, W.C., et al.,** ***Requirement for Casper (c-FLIP) in regulation of death receptor-induced apoptosis and embryonic development.*** **Immunity, 2000. 12(6): p. 633-42.**
26. **Su, H., et al.,** ***Requirement for caspase-8 in NF-kappaB activation by antigen receptor.*** **Science, 2005. 307(5714): p. 1465-8.**
27. **Scaffidi, C., et al.,** ***Two CD95 (APO-1/Fas) signaling pathways.*** **EMBO J, 1998. 17(6): p. 1675-87.**
28. **Li, H., et al.,** ***Cleavage of BID by caspase 8 mediates the mitochondrial damage in the Fas pathway of apoptosis.*** **Cell, 1998. 94(4): p. 491-501.**
29. **Muppidi, J.R. and R.M. Siegel,** ***Ligand-independent redistribution of Fas (CD95) into lipid rafts mediates clonotypic T cell death.*** **Nat Immunol, 2004. 5(2): p. 182-9.**
30. **Siegel, R.M., et al.,** ***Fas preassociation required for apoptosis signaling and dominant inhibition by pathogenic mutations.*** **Science, 2000. 288(5475): p. 2354-7.**
31. **Feig, C., et al.,** ***Palmitoylation of CD95 facilitates formation of SDS-stable receptor aggregates that initiate apoptosis signaling.*** **EMBO J, 2007. 26(1): p. 221-31.**
32. **Misra, R.S., et al.,** ***Caspase-8 and c-FLIPL associate in lipid rafts with NF-kappaB adaptors during T cell activation.*** **J Biol Chem, 2007. 282(27): p. 19365-74.**
33. **Stegh, A.H., et al.,** ***Identification of the cytolinker plectin as a major early in vivo substrate for caspase 8 during CD95- and tumor necrosis factor receptor-mediated apoptosis.*** **Mol Cell Biol, 2000. 20(15): p. 5665-79.**
34. **Chandra, D., et al.,** ***Association of active caspase 8 with the mitochondrial membrane during apoptosis: potential roles in cleaving BAP31 and caspase 3 and mediating***

mitochondrion-endoplasmic reticulum cross talk in etoposide-induced cell death. **Mol Cell Biol, 2004. 24(15): p. 6592-607.**

35. **Gonzalvez, F., et al.,** ***Cardiolipin provides an essential activating platform for caspase-8 on mitochondria.*** **J Cell Biol, 2008. 183(4): p. 681-96.**
36. **Schug, Z.T. and E. Gottlieb,** ***Cardiolipin acts as a mitochondrial signalling platform to launch apoptosis.*** **Biochim Biophys Acta, 2009. 1788(10): p. 2022-31.**
37. **Lutter, M., et al.,** ***Cardiolipin provides specificity for targeting of tBid to mitochondria.*** **Nat Cell Biol, 2000. 2(10): p. 754-61.**
38. **Kuwana, T., et al.,** ***Bid, Bax, and lipids cooperate to form supramolecular openings in the outer mitochondrial membrane.*** **Cell, 2002. 111(3): p. 331-42.**
39. **Scorrano, L.,** ***Caspase-8 goes cardiolipin: a new platform to provide mitochondria with microdomains of apoptotic signals?*** **J Cell Biol, 2008. 183(4): p. 579-81.**
40. **Ng, F.W., et al.,** ***p28 Bap31, a Bcl-2/Bcl-XL- and procaspase-8-associated protein in the endoplasmic reticulum.*** **J Cell Biol, 1997. 139(2): p. 327-38.**
41. **Breckenridge, D.G., et al.,** ***The procaspase-8 isoform, procaspase-8L, recruited to the BAP31 complex at the endoplasmic reticulum.*** **Proc Natl Acad Sci U S A, 2002. 99(7): p. 4331-6.**
42. **Krajewski, S., et al.,** ***Investigation of the subcellular distribution of the bcl-2 oncoprotein: residence in the nuclear envelope, endoplasmic reticulum, and outer mitochondrial membranes.*** **Cancer Res, 1993. 53(19): p. 4701-14.**
43. **Wang, B., et al.,** ***Uncleaved BAP31 in association with A4 protein at the endoplasmic reticulum is an inhibitor of Fas-initiated release of cytochrome c from mitochondria.*** **J Biol Chem, 2003. 278(16): p. 14461-8.**
44. **Breckenridge, D.G., et al.,** ***Caspase cleavage product of BAP31 induces mitochondrial fission through endoplasmic reticulum calcium signals, enhancing cytochrome c release to the cytosol.*** **J Cell Biol, 2003. 160(7): p. 1115-27.**
45. **Wozniak, A.L., et al.,** ***Requirement of biphasic calcium release from the endoplasmic reticulum for Fas-mediated apoptosis.*** **J Cell Biol, 2006. 175(5): p. 709-14.**
46. **Gomez-Angelats, M. and J.A. Cidlowski,** ***Molecular evidence for the nuclear localization of FADD.*** **Cell Death Differ, 2003. 10(7): p. 791-7.**
47. **Xiang, R., et al.,** ***Adaptor FADD is recruited by RTN3/HAP in ER-bound signaling complexes.*** **Apoptosis, 2006. 11(11): p. 1923-32.**
48. **Teng, F.Y. and B.L. Tang,** ***Cell autonomous function of Nogo and reticulons: The emerging story at the endoplasmic reticulum.*** **J Cell Physiol, 2008. 216(2): p. 303-8.**
49. **Browman, D.T., et al.,** ***Erlin-1 and erlin-2 are novel members of the prohibitin family of proteins that define lipid-raft-like domains of the ER.*** **J Cell Sci, 2006. 119(Pt 15): p. 3149-60.**

50. **Sorice, M., et al.,** ***Cardiolipin-enriched raft-like microdomains are essential activating platforms for apoptotic signals on mitochondria.*** **FEBS Lett, 2009. 583(15): p. 2447-50.**

51. **Sorice, M., et al.,** ***Dynamics of mitochondrial raft-like microdomains in cell life and death.*** **Commun Integr Biol, 2012. 5(2): p. 217-9.**

52. **Vance, J.E.,** ***Phospholipid synthesis in a membrane fraction associated with mitochondria.*** **J Biol Chem, 1990. 265(13): p. 7248-56.**

53. **Hayashi, T. and M. Fujimoto,** ***Detergent-resistant microdomains determine the localization of sigma-1 receptors to the endoplasmic reticulum-mitochondria junction.*** **Mol Pharmacol, 2010. 77(4): p. 517-28.**

54. **Area-Gomez, E., et al.,** ***Upregulated function of mitochondria-associated ER membranes in Alzheimer disease.*** **EMBO J, 2012.**

55. **Poston, C.N., et al.,** ***Proteomic analysis of lipid raft-enriched membranes isolated from internal organelles.*** **Biochem Biophys Res Commun, 2011. 415(2): p. 355-60.**

56. **Lamarca, V. and L. Scorrano,** ***When separation means death: killing through the mitochondria, but starting from the endoplasmic reticulum.*** **EMBO J, 2009. 28(12): p. 1681-3.**

57. **Pinton, P., et al.,** ***Reduced loading of intracellular Ca(2+) stores and downregulation of capacitative Ca(2+) influx in Bcl-2-overexpressing cells.*** **J Cell Biol, 2000. 148(5): p. 857-62.**

58. **Scorrano, L., et al.,** ***BAX and BAK regulation of endoplasmic reticulum Ca2+: a control point for apoptosis.*** **Science, 2003. 300(5616): p. 135-9.**

59. **Porter, K.R., A. Claude, and E.F. Fullam,** ***A Study of Tissue Culture Cells by Electron Microscopy : Methods and Preliminary Observations.*** **J Exp Med, 1945. 81(3): p. 233-46.**

60. **Palade, G.E. and P. Siekevitz,** ***Liver microsomes; an integrated morphological and biochemical study.*** **J Biophys Biochem Cytol, 1956. 2(2): p. 171-200.**

61. **Watson, M.L.,** ***The nuclear envelope; its structure and relation to cytoplasmic membranes.*** **J Biophys Biochem Cytol, 1955. 1(3): p. 257-70.**

62. **Voeltz, G.K., M.M. Rolls, and T.A. Rapoport,** ***Structural organization of the endoplasmic reticulum.*** **EMBO Rep, 2002. 3(10): p. 944-50.**

63. **Lynes, E.M. and T. Simmen,** ***Urban planning of the endoplasmic reticulum (ER): how diverse mechanisms segregate the many functions of the ER.*** **Biochim Biophys Acta, 2011. 1813(10): p. 1893-905.**

64. **Palade, G.E.,** ***The endoplasmic reticulum.*** **J Biophys Biochem Cytol, 1956. 2(4 Suppl): p. 85-98.**

65. **English, A.R., N. Zurek, and G.K. Voeltz,** ***Peripheral ER structure and function.*** **Curr Opin Cell Biol, 2009. 21(4): p. 596-602.**

66. **Gilham, D., et al.,** ***Triacylglycerol hydrolase is localized to the endoplasmic reticulum by an unusual retrieval sequence where it participates in VLDL assembly without utilizing VLDL lipids as substrates.*** **Mol Biol Cell, 2005. 16(2): p. 984-96.**

67. **Satoh, T., et al.,** ***The inositol 1,4,5,-trisphosphate receptor in cerebellar Purkinje cells: quantitative immunogold labeling reveals concentration in an ER subcompartment.*** **J Cell Biol, 1990. 111(2): p. 615-24.**

68. **Golovina, V.A. and M.P. Blaustein,** ***Spatially and functionally distinct Ca2+ stores in sarcoplasmic and endoplasmic reticulum.*** **Science, 1997. 275(5306): p. 1643-8.**

69. **Berridge, M.J.,** ***The endoplasmic reticulum: a multifunctional signaling organelle.*** **Cell Calcium, 2002. 32(5-6): p. 235-49.**

70. **Friedman, J.R. and G.K. Voeltz,** ***The ER in 3D: a multifunctional dynamic membrane network.*** **Trends Cell Biol, 2011. 21(12): p. 709-17.**

71. **Voeltz, G.K., et al.,** ***A class of membrane proteins shaping the tubular endoplasmic reticulum.*** **Cell, 2006. 124(3): p. 573-86.**

72. **Shibata, Y., et al.,** ***Mechanisms shaping the membranes of cellular organelles.*** **Annu Rev Cell Dev Biol, 2009. 25: p. 329-54.**

73. **Shibata, Y., et al.,** ***The reticulon and DP1/Yop1p proteins form immobile oligomers in the tubular endoplasmic reticulum.*** **J Biol Chem, 2008. 283(27): p. 18892-904.**

74. **Hu, J., et al.,** ***A class of dynamin-like GTPases involved in the generation of the tubular ER network.*** **Cell, 2009. 138(3): p. 549-61.**

75. **Orso, G., et al.,** ***Homotypic fusion of ER membranes requires the dynamin-like GTPase atlastin.*** **Nature, 2009. 460(7258): p. 978-83.**

76. **Shibata, Y., et al.,** ***Mechanisms determining the morphology of the peripheral ER.*** **Cell, 2010. 143(5): p. 774-88.**

77. **Lin, S., S. Sun, and J. Hu,** ***Molecular basis for sculpting the endoplasmic reticulum membrane.*** **Int J Biochem Cell Biol, 2012. 44(9): p. 1436-43.**

78. **West, M., et al.,** ***A 3D analysis of yeast ER structure reveals how ER domains are organized by membrane curvature.*** **J Cell Biol, 2011. 193(2): p. 333-46.**

79. **Pichler, H., et al.,** ***A subfraction of the yeast endoplasmic reticulum associates with the plasma membrane and has a high capacity to synthesize lipids.*** **Eur J Biochem, 2001. 268(8): p. 2351-61.**

80. **Park, C.Y., et al.,** ***STIM1 clusters and activates CRAC channels via direct binding of a cytosolic domain to Orai1.*** **Cell, 2009. 136(5): p. 876-90.**

81. **Orci, L., et al.,** ***From the Cover: STIM1-induced precortical and cortical subdomains of the endoplasmic reticulum.*** **Proc Natl Acad Sci U S A, 2009. 106(46): p. 19358-62.**

82. **Levine, T. and C. Loewen,** ***Inter-organelle membrane contact sites: through a glass, darkly.*** **Curr Opin Cell Biol, 2006. 18(4): p. 371-8.**

83. Hoepfner, D., et al., *Contribution of the endoplasmic reticulum to peroxisome formation.* Cell, 2005. 122(1): p. 85-95.

84. Wanders, R.J., et al., *Peroxisomes, lipid metabolism and lipotoxicity.* Biochim Biophys Acta, 2010. 1801(3): p. 272-80.

85. Copeland, D.E. and A.J. Dalton, *An association between mitochondria and the endoplasmic reticulum in cells of the pseudobranch gland of a teleost.* J Biophys Biochem Cytol, 1959. 5(3): p. 393-6.

86. Lewis, J.A. and J.R. Tata, *A rapidly sedimenting fraction of rat liver endoplasmic reticulum.* J Cell Sci, 1973. 13(2): p. 447-59.

87. Csordas, G., et al., *Structural and functional features and significance of the physical linkage between ER and mitochondria.* J Cell Biol, 2006. 174(7): p. 915-21.

88. Rizzuto, R., et al., *Close contacts with the endoplasmic reticulum as determinants of mitochondrial Ca2+ responses.* Science, 1998. 280(5370): p. 1763-6.

89. Rizzuto, R., et al., *Microdomains with high Ca2+ close to IP3-sensitive channels that are sensed by neighboring mitochondria.* Science, 1993. 262(5134): p. 744-7.

90. de Brito, O.M. and L. Scorrano, *An intimate liaison: spatial organization of the endoplasmic reticulum-mitochondria relationship.* EMBO J, 2010. 29(16): p. 2715-23.

91. Giorgi, C., et al., *Structural and functional link between the mitochondrial network and the endoplasmic reticulum.* Int J Biochem Cell Biol, 2009. 41(10): p. 1817-27.

92. Myhill, N., et al., *The subcellular distribution of calnexin is mediated by PACS-2.* Mol Biol Cell, 2008. 19(7): p. 2777-88.

93. Hayashi, T. and T.P. Su, *Sigma-1 receptor chaperones at the ER-mitochondrion interface regulate Ca(2+) signaling and cell survival.* Cell, 2007. 131(3): p. 596-610.

94. Lynes, E.M., et al., *Palmitoylated TMX and calnexin target to the mitochondria-associated membrane.* EMBO J, 2012. 31(2): p. 457-70.

95. Gilady, S.Y., et al., *Ero1alpha requires oxidizing and normoxic conditions to localize to the mitochondria-associated membrane (MAM).* Cell Stress Chaperones, 2010. 15(5): p. 619-29.

96. Area-Gomez, E., et al., *Presenilins are enriched in endoplasmic reticulum membranes associated with mitochondria.* Am J Pathol, 2009. 175(5): p. 1810-6.

97. Urano, Y., et al., *Association of active gamma-secretase complex with lipid rafts.* J Lipid Res, 2005. 46(5): p. 904-12.

98. de Brito, O.M. and L. Scorrano, *Mitofusin 2 tethers endoplasmic reticulum to mitochondria.* Nature, 2008. 456(7222): p. 605-10.

99. Anesti, V. and L. Scorrano, *The relationship between mitochondrial shape and function and the cytoskeleton.* Biochim Biophys Acta, 2006. 1757(5-6): p. 692-9.

100. **Cerqua, C., et al.,** ***Trichoplein/mitostatin regulates endoplasmic reticulum-mitochondria juxtaposition.*** **EMBO Rep, 2010. 11(11): p. 854-60.**

101. **Kornmann, B., et al.,** ***An ER-mitochondria tethering complex revealed by a synthetic biology screen.*** **Science, 2009. 325(5939): p. 477-81.**

102. **Rowland, A.A. and G.K. Voeltz,** ***Endoplasmic reticulum-mitochondria contacts: function of the junction.*** **Nat Rev Mol Cell Biol, 2012. 13(10): p. 607-25.**

103. **Simmen, T., et al.,** ***PACS-2 controls endoplasmic reticulum-mitochondria communication and Bid-mediated apoptosis.*** **EMBO J, 2005. 24(4): p. 717-29.**

104. **Szabadkai, G., et al.,** ***Chaperone-mediated coupling of endoplasmic reticulum and mitochondrial Ca2+ channels.*** **J Cell Biol, 2006. 175(6): p. 901-11.**

105. **Raturi, A. and T. Simmen,** ***Where the endoplasmic reticulum and the mitochondrion tie the knot: The mitochondria-associated membrane (MAM).*** **Biochim Biophys Acta, 2012.**

106. **Rizzuto, R., et al.,** ***Ca(2+) transfer from the ER to mitochondria: when, how and why.*** **Biochim Biophys Acta, 2009. 1787(11): p. 1342-51.**

107. **Patergnani, S., et al.,** ***Calcium signaling around Mitochondria Associated Membranes (MAMs).*** **Cell Commun Signal, 2011. 9: p. 19.**

108. **Pinton, P., et al.,** ***Calcium and apoptosis: ER-mitochondria Ca2+ transfer in the control of apoptosis.*** **Oncogene, 2008. 27(50): p. 6407-18.**

109. **Szegezdi, E., et al.,** ***Bcl-2 family on guard at the ER.*** **Am J Physiol Cell Physiol, 2009. 296(5): p. C941-53.**

110. **Chen, R., et al.,** ***Bcl-2 functionally interacts with inositol 1,4,5-trisphosphate receptors to regulate calcium release from the ER in response to inositol 1,4,5-trisphosphate.*** **J Cell Biol, 2004. 166(2): p. 193-203.**

111. **Marchi, S., et al.,** ***Akt kinase reducing endoplasmic reticulum Ca2+ release protects cells from Ca2+-dependent apoptotic stimuli.*** **Biochem Biophys Res Commun, 2008. 375(4): p. 501-5.**

112. **Giorgi, C., et al.,** ***PML regulates apoptosis at endoplasmic reticulum by modulating calcium release.*** **Science, 2010. 330(6008): p. 1247-51.**

113. **Tabas, I. and D. Ron,** ***Integrating the mechanisms of apoptosis induced by endoplasmic reticulum stress.*** **Nat Cell Biol, 2011. 13(3): p. 184-90.**

114. **Hetz, C.,** ***The unfolded protein response: controlling cell fate decisions under ER stress and beyond.*** **Nat Rev Mol Cell Biol, 2012. 13(2): p. 89-102.**

115. **Klee, M., et al.,** ***Mitochondrial apoptosis induced by BH3-only molecules in the exclusive presence of endoplasmic reticular Bak.*** **EMBO J, 2009. 28(12): p. 1757-68.**

116. **Manders, E.M., Verbeek, F. J. and Aten, J. A.,** ***Measurement of co-localisation of objects in dual-colour confocal images.*** **Journal of Microscopy, 1993. 169(3): p. 375-382**

117. **Sriburi, R., et al.,** ***XBP1: a link between the unfolded protein response, lipid biosynthesis, and biogenesis of the endoplasmic reticulum.*** **J Cell Biol, 2004. 167(1): p. 35-41.**

118. **Schuck, S., et al.,** ***Membrane expansion alleviates endoplasmic reticulum stress independently of the unfolded protein response.*** **J Cell Biol, 2009. 187(4): p. 525-36.**

119. **Shain, K.H., T.H. Landowski, and W.S. Dalton,** ***Adhesion-mediated intracellular redistribution of c-Fas-associated death domain-like IL-1-converting enzyme-like inhibitory protein-long confers resistance to CD95-induced apoptosis in hematopoietic cancer cell lines.*** **J Immunol, 2002. 168(5): p. 2544-53.**

120. **Voss, C., et al.,** ***ER-shaping proteins facilitate lipid exchange between the ER and mitochondria in S. cerevisiae.*** **J Cell Sci, 2012.**

121. **Verfaillie, T., et al.,** ***PERK is required at the ER-mitochondrial contact sites to convey apoptosis after ROS-based ER stress.*** **Cell Death Differ, 2012. 19(11): p. 1880-91.**

122. **Schweigreiter, R., et al.,** ***Phosphorylation-regulated cleavage of the reticulon protein Nogo-B by caspase-7 at a noncanonical recognition site.*** **Proteomics, 2007. 7(24): p. 4457-67.**

123. **Chandler, J.M., G.M. Cohen, and M. MacFarlane,** ***Different subcellular distribution of caspase-3 and caspase-7 following Fas-induced apoptosis in mouse liver.*** **J Biol Chem, 1998. 273(18): p. 10815-8.**

124. **Frezza, C., S. Cipolat, and L. Scorrano,** ***Organelle isolation: functional mitochondria from mouse liver, muscle and cultured fibroblasts.*** **Nat Protoc, 2007. 2(2): p. 287-95.**

125. **Mosmann, T.,** ***Rapid colorimetric assay for cellular growth and survival: application to proliferation and cytotoxicity assays.*** **J Immunol Methods, 1983. 65(1-2): p. 55-63.**

126. **Grynkiewicz, G., M. Poenie, and R.Y. Tsien,** ***A new generation of Ca2+ indicators with greatly improved fluorescence properties.*** **J Biol Chem, 1985. 260(6): p. 3440-50.**